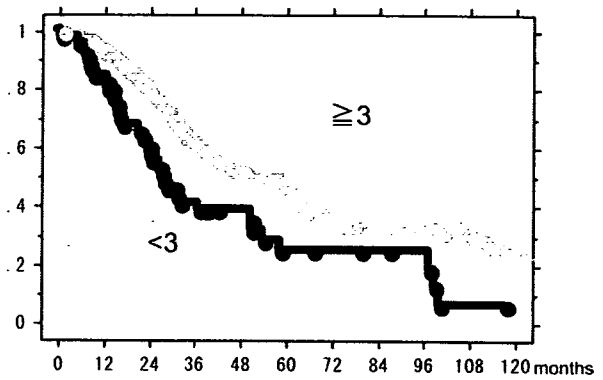

Figure 1. Overall survival curves according to PSA/PAP ratio.

Table 2. Univariate analysis of prognostic factors

Variable	*P* Value
Age (≥75 vs. <75 yr)	0.1362
Performance status (0, 1, 2 vs. 3, 4)	0.8609
Symptoms (yes vs. no)	0.2007
Hb (≥12 vs. <12 g/dL)	0.0244*
Plt (≥15 vs. <15 × 104/μL)	0.1223
ALP (≥500 vs. <500 IU/L)	0.0003*
LDH (≥400 vs. <400 IU/L)	0.0030*
T stage (<T3a vs. ≥T3a)	0.4369
N stage (N0 vs. N1)	0.9409
M stage (M1ab vs. M1c)	0.8551
EOD (0, 1 vs. 2, 3, 4)	0.0054*
Histologic differentiation (well vs. moderate, poor)	0.3292
PSA (≥100 vs. <100 ng/mL)	0.3558
PAP (≥30 vs. <30 ng/mL)	0.9872
PSA/PAP ratio (≥3 vs. <3)	0.0055*

Hb = hemoglobin; Plt = platelets; ALP = alkaline phosphatase; LDH = lactate dehydrogenase; other abbreviations as in Table 1.

48.0% for those with a PSA/PAP ratio of less than 3.0 and 3.0 or greater, respectively (Fig. 1).

Outcomes According to Univariate and Multivariate Analyses

The univariate analysis results of the prognostic factors are given in Table 2. Anemia, high alkaline phosphatase, high lactate dehydrogenase, high extent of disease in bone metastasis,[18] and low PSA/PAP ratio correlated significantly with poor survival. Subsequently, we undertook a multivariate analysis with the variables that were significant on univariate analysis (Table 3). The statistically significant prognostic factors for overall survival were alkaline phosphatase (P = 0.0413), lactate dehydrogenase (P = 0.0409), and PSA/PAP ratio (P = 0.0113).

COMMENT

The clinical significance of the pretreatment serum PSA values studied by Kuriyama *et al.*[16] indicated that serum PSA measurement can be used to predict the prognosis of patients with prostate cancer. However, it has been determined that poorly differentiated prostate cancer expresses significantly less PSA than does benign prostatic glands or low-grade adenocarcinoma cells.[14,15] Consequently, highly malignant prostate cancer frequently shows comparatively low PSA levels, and a low PSA level does not always indicate a good prognosis for patients with advanced prostate cancer.

Another significant tumor marker of the prostate is acid phosphatase. Acid phosphatase is the first tumor marker in epithelial tumors, and PAP is a subtype of acid phosphatase. According to the genotypes, acid phosphatase is composed of four isoforms.[20] The erythrocytic and lysosomal forms are expressed in most cells. In contrast, the prostatic and macrophage forms have more limited expression. In the middle of the 1930s, Gutman *et al.*[21] made a noteworthy observation that the activity of PAP is increased in the circulation of patients with prostate cancer, especially those with bone metastasis, compared with healthy adults. Subsequently, it was established that the PAP activity in the circulation of patients with prostate cancer correlates with prostate cancer progression and could serve as an indicator of treatment response.[22,23] Thus, PAP was the biochemical diagnostic mainstay for prostate cancer until the advent of PSA. PSA improved the detection of early-stage prostate cancer, because PAP is not elevated in most early prostate cancer cases.

In contrast, positive rates of PAP in metastatic prostate cancer are as high as those of PSA. Both PSA and PAP are serologic markers specific for prostatic tissue, but not for cancer tissue. Moreover, highly malignant dedifferentiated cancer can be associated with less-expressed PSA and PAP. PAP expression might be relatively maintained in the process of dedifferentiation, which could explain why the PSA/PAP ratio is low in highly malignant, poorly differentiated prostate cancer. However, Grande *et al.*[24] reported lower tissue PAP levels in metastatic cancer compared with localized cancer, as well as lower tissue PSA levels in metastatic cancer compared with localized cancer, and the difference was more significant for PAP. We consider this result was true between the tissue level of metastatic and nonmetastatic disease, but, as examined, for these molecules in the sera within metastatic cases, the reduction of PSA is possibly prominent.

Morote *et al.*[25] reported that a PSA/PAP ratio of less than 1 (inversion of PSA/PAP) was a definite indicator of metastatic prostate cancer and, also, that this cutoff was relevant to the prognosis. However, the fraction of patients with this criterion was extremely small, and as stressed by the investigators, it accounted for only 3.2% of patients with prostate cancer. In addition, they did not undertake theoretical survival analyses and failed to show the PSA/PAP ratio as an independent prognostic factor.[25] The present study demonstrated that a PSA/PAP ratio of less than 3 is an independent index, and the

Table 3. Multivariate analysis of prognostic factors

Variable	Hazard Ratio	95% CI	P Value
Hb (≥12 vs. <12 g/dL)	0.803	0.536–1.203	0.2871
ALP (≥500 vs. <500 IU/L)	1.571	1.018–2.425	0.0413
LDH (≥400 vs. <400 IU/L)	1.619	1.020–2.568	0.0409
EOD (0, 1 vs. 2, 3, 4)	0.747	0.497–1.122	0.1602
PSA/PAP (≥3 vs. <3)	1.723	1.131–2.623	0.0113

CI = confidence interval; other abbreviations as in Tables 1 and 2.

statistical approach confirmed that the results with this value are reproducible even within the Stage IV cases.

CONCLUSIONS

The results of our study have indicated that the PSA/PAP ratio is a valuable prognostic indicator in men with Stage IV prostate cancer. Although our study found that other laboratory tests also have prognostic influence, the PSA/PAP ratio was an essential index implicated in the physiopathology of prostate cancer. Although Moul *et al.*[26] advocated the contemporary value of PAP, it is becoming a remnant of the past.[27] With the results of the present study, however, PAP might become more useful when analyzed in conjunction with the PSA level.[19]

Acknowledgment. To Dr. Yasunosuke Sakata, Manabu Watanabe, Norio Miyajima, Masaaki Naito, Naoki Arimoto, Toshiyuki Itoi, Kazuhiro Kobayashi, Kazuya Suzuki, Etsuko Isahaya, Shuichi Komatsu, and Takashi Kasahara for their enthusiastic contribution to the treatment of the patients in this study.

References

1. Badalament RA, and Drago JR: Prostate cancer. Dis Mon **37:** 199–268, 1991.
2. Greenlee RT, Hill-Harmon MB, Murray T, *et al:* Cancer statistics 2001. CA Cancer J Clin **51:** 15–36, 2001.
3. Yoshimi I, and Sobue T: Current status and trends in cancer mortality in Japan. Jpn J Cancer Chemother **31:** 832–839, 2004.
4. Cancer Registration Committee of the Japanese Urological Association: Clinicopathological statistics on registered prostate cancer patients in Japan: 2000 report from the Japanese Urological Association. Int J Urol **12:** 46–61, 2005.
5. Saito T, Kitamura Y, Komatsubara S, *et al:* Outcomes of locally advanced prostate cancer: a single institution study of 209 patients in Japan. Asian J Androl **8:** 555–561, 2006.
6. Saito T, Kitamura Y, and Komatsubara S: Chemo-endocrine therapy for newly diagnosed stage D2 prostate cancer. Hinyokika Kiyo **51:** 789–792, 2005.
7. Mulders PF, Dijkman GA, Fernandez del Moral P, *et al:* for the Dutch Southeastern Urological Cooperative Group: Analysis of prognostic factors in disseminated prostatic cancer: an update. Cancer **65:** 2758–2761, 1990.
8. Eisenberger MA, Crawford ED, Wolf M, *et al:* Prognostic factors in stage D2 prostate cancer: important implications for future trials—results of a cooperative Intergroup study (INT 0036). The National Cancer Institute Intergroup Study #0036. Semin Oncol **21:** 613–619, 1994.
9. Vollmer RT, Kantoff PW, Dawson NA, *et al:* A prognostic score for hormone-refractory prostate cancer: analysis of two cancer and leukemia group B studies. Clin Cancer Res **5:** 831–837, 1999.
10. Halabi S, Small EJ, Kantoff PW, *et al:* Prognostic model for predicting survival in men with hormone-refractory metastatic prostate cancer. J Clin Oncol **21:** 1232–1237, 2003.
11. Rozhansky F, Chen MH, Cox MC, *et al:* Prostate-specific antigen velocity and survival for patients with hormone-refractory metastatic prostate carcinoma. Cancer **106:** 63–67, 2006.
12. Hara N, Kitamura Y, Saito T, *et al:* Total and free prostate-specific antigen indexes in prostate cancer screening: value and limitation for Japanese populations. Asian J Androl **8:** 429–434, 2006.
13. Roscigno M, Scattoni V, Bertini R, *et al:* Diagnosis of prostate cancer: state of the art. Minerva Urol Nefrol **56:** 123–145, 2004.
14. Varma M, Morgan M, Jasani MB, *et al:* Polyclonal anti-PSA is more sensitive but less specific than monoclonal anti-PSA: implications for diagnostic prostatic pathology. Am J Clin Pathol **118:** 202–207, 2002.
15. Goldstein NS: Immunophenotypic characterization of 225 prostate adenocarcinomas with intermediate or high Gleason scores. Am J Clin Pathol **117:** 471–477, 2002.
16. Kuriyama M, Akimoto S, Akaza H, *et al:* Comparison of various assay systems for prostate-specific antigen standardization. Jpn J Clin Oncol **22:** 393–399, 1992.
17. Jibiki K, Momura T, Demura R, *et al:* Fundamental and clinical studies on PAP "Eiken" kit. Clin Endocrinol **29:** 1547–1552, 1981.
18. Soloway MS, Hardeman SW, Hickey D, *et al:* Stratification of patients with metastatic prostate cancer based on extent of disease on initial bone scan. Cancer **61:** 195–202, 1988.
19. Kuriyama M, Obata K, Miyagawa Y, *et al:* Serum prostate-specific antigen values for the prediction of clinical stage and prognosis in patients with prostate cancer: an analysis of 749 cases. Int J Urol **3:** 462–467, 1996.
20. Moss DW, Raymond FD, and Wile DB: Clinical and biological aspects of acid phosphatase. Crit Rev Clin Lab Sci **32:** 431–467, 1995.
21. Gutman EB, Sproul EE, and Gutman AB: Significance of increased phosphatase activity at the site of osteoplastic metastases secondary to carcinoma of the prostate gland. Am J Cancer **28:** 485–495, 1936.
22. Huggins C, and Hodges CV: Studies on prostatic cancer: the effect of castration, of estrogen and of androgen injection on serum phosphatases in metastatic carcinoma of the prostate. Cancer Res **1:** 293–297, 1941.
23. Veeramani S, Yuan TC, Chen SJ, *et al:* Cellular prostatic acid phosphatase: a protein tyrosine phosphatase involved in androgen-independent proliferation of prostate cancer. Endocr Relat Cancer **12:** 805–822, 2005.
24. Grande M, Carlstrom K, Lundh-Rozell B, *et al:* Changes in tissue prostatic acidic phosphatase during endocrine treatment of patients with prostatic carcinoma. Scand J Urol Nephrol **39:** 393–398, 2005.
25. Morote J, Vallejo C, and Lorente JA: Clinical significance of inverted PSA/PAP ratio in prostate cancer patients. Int J Biol Markers **10:** 58, 1995.
26. Moul JW, Connelly RR, Perahia B, *et al:* The contemporary value of pretreatment prostatic acid phosphatase to predict pathological stage and recurrence in radical prostatectomy cases. J Urol **159:** 935–940, 1998.
27. Saito T, Kitamura Y, and Komatsubara S: Prognosis of prostate cancer with elevated prostatic acid phosphatase Hinyokika Kiyo **52:** 177–180, 2006.

Int. J. Cancer: **122**, 39–49 (2008)

Glycosylation status of haptoglobin in sera of patients with prostate cancer *vs.* benign prostate disease or normal subjects

Tsutomu Fujimura[1], Yasuro Shinohara[2], Bérangère Tissot[3], Poh-Choo Pang[3], Masaki Kurogochi[2], Seiichi Saito[4], Yoichi Arai[4], Martin Sadilek[5], Kimie Murayama[1], Anne Dell[3]*, Shin-Ichiro Nishimura[2]* and Sen-Itiroh Hakomori[1,6]*

[1]*Department of Pathobiology, University of Washington and Pacific Northwest Research Institute, 720 Broadway, Seattle, WA*
[2]*Laboratory of Advanced Chemical Biology, Graduate School of Advanced Life Science, Hokkaido University N21, W11, Kita-ku, Sapporo 001, Japan*
[3]*Division of Molecular Biosciences, Faculty of Natural Sciences, Imperial College London, London SW7 2AZ, United Kingdom*
[4]*Department of Urology, Tohoku University School of Medicine, Seiryo-machi, Aoba-ku, Sendai 980, Japan*
[5]*Department of Chemistry, University of Washington and Pacific Northwest Research Institute, 720 Broadway, Seattle, WA*
[6]*Department of Microbiology, University of Washington, and Pacific Northwest Research Institute 720 Broadway, Seattle, WA*

We studied chemical level and glycosylation status of haptoglobin in sera of patients with prostate cancer, as compared to benign prostate disease and normal subjects, with the following results. (*i*) Haptoglobin level was enhanced significantly in sera of prostate cancer. (*ii*) Sialylated bi-antennary glycans were the dominant structures in haptoglobins from all 3 sources, regardless of different site of N-linked glycan. The N-linked glycans at N184 were exclusively bi-antennary, and showed no difference between prostate cancer *vs.* benign prostate disease. (*iii*) Tri-antennary, N-linked, fucosylated glycans, carrying at least 1 sialyl-Lewis$^{x/a}$ antenna, were predominantly located on N207 or N211 within the amino acid 203-215 sequence of the β-chain of prostate cancer, and were minimal in benign prostate disease. Fucosylated glycans were not observed in normal subjects. A minor tri-antennary N-linked glycan was observed at N241 of the β-chain in prostate cancer, which was absent in benign prostate disease. (*iv*) None of these N-linked structures showed the expected presence of disialylated antennae with GalNAcβ4(NeuAcα3)Galβ3(NeuAcα6)GlcNAcβGal, or its analogue, despite cross-reactivity of prostate cancer haptoglobin with monoclonal antibody RM2. (*v*) Minor levels of *O*-glycosylation were identified in prostate cancer haptoglobin for the first time. Mono- and disialyl core Type 1 O-linked structures were identified after reductive β-elimination followed by methylation and mass spectrometric analysis. No evidence was found for the presence of specific RM2 or other tumor-associated glycosyl epitopes linked to this *O*-glycan core. In summary, levels of haptoglobin are enhanced in sera of prostate cancer patients, and the *N*-glycans attached to a defined peptide region of its β-chain are characterized by enhanced branching as well as antenna fucosylation.

Key words: *N*-glycosylation; tri-antennary; haptoglobin; beta-chain; alpha2-chain; glycopeptides; antenna fucosylation

Aberrant glycosyl epitopes, defined by specific monoclonal antibodies (mAbs), in glycolipids and glycoproteins have been regarded as useful biomarkers for cancer diagnosis,[1] and in some cases for cancer therapy[2–4]; for review see Ref. 5. Out of many glycosyl epitopes, lacto-series Type 1 chain structures Le^c,[6,7] sialyl-Le^a,[8] disialyl-Lc4,[9] and dimeric-Le^a,[10,11] and O-linked Tn[12,13] and sialyl-Tn,[14,15] have often been regarded as useful biomarkers. The antigen GalNAcβ4-disialyl-Lc4,[16] defined by mAb RM2, was found to react with prostate cancer tissue, but not with benign prostate disease or normal prostate gland.[17]

Haptoglobin, a hemoglobin-binding glycoprotein, is a major serum component, consisting of β-, α1- and α2-chains, which are disulfide-linked together in various combinations. Differences in subunit combination pattern give rise to a large variety of haptoglobin polymorphism patterns in serum. In addition, the haptoglobin chemical level in serum increases significantly in association with inflammation, cancer development, and some physiological processes (for review see Refs. 18 and 19).

While there are 4 consensus sequences for *N*-glycosylation sites in the β-chain of haptoglobin, none is located in the α-chain. During the past decade, the *N*-glycosylation status of haptoglobin, with particular focus on changes of fucosylation and sialylation associated with many diseases has been extensively studied, since haptoglobin is regarded as an "acute-phase protein" and is elevated in many diseases (see Discussion).

In view of recent progress, particularly with glycomics approach by mass spectrometry, regarding glycosylation status of haptoglobin associated with various types of cancer (see Discussion), and the lack of such studies on prostate cancer haptoglobin, we performed the following studies: (*i*) Comparison of haptoglobin levels in sera of prostate cancer patients with levels in benign prostate disease and normal subjects. (*ii*) Mass spectrometric analysis of tryptic glycopeptides obtained from haptoglobin which was affinity-purified through a hemoglobin-Sepharose column. (*iii*) Mass spectrometric analysis of N-linked glycans released by PNGase-F from haptoglobin β-chain. (*iv*) Mass spectrometric analysis of O-linked glycans released by reductive β-elimination of affinity-purified haptoglobin.

Our results indicate that N-linked, tri-antennary glycans carrying 1 or more SLe$^{x/a}$ antennae in 1 *N*-glycosylation domain of the haptoglobin β-chain are highly expressed in prostate cancer patients, but minimal in benign prostate disease or normal subjects. Additionally, we show that prostate cancer haptoglobin carries a low level of *O*-glycosylation, but that no specific glycosyl epitope such as RM2 or its analogue is detectable by the mass spectrometric methods employed, in either N-linked or O-linked glycans in the β- or α-chain of haptoglobin.

Abbreviations: aoWR, N^{α}-((aminooxy)acetyl)tryptophanylarginine methyl ester; GalNAc, *N*-acetylgalactosamine; GlcNAc, *N*-acetylglucosamine; HPLC, high-performance liquid chromatography; mAb, monoclonal antibody; MALDI-TOF MS, matrix assisted laser desorption/ionization time-of-flight mass spectrometry; PBS (-), phosphate-buffered saline (-), *i.e.*, 0.15 M NaCl, 20 mM of a mixture of Na_2HPO_4/NaH_2PO_4, pH adjusted to 7.2, without addition of Ca^{2+} or Mg^{2+}); PNGase-F, peptide-*N*4-(acetyl-β-glucosaminyl)-asparagine amidase; RM2 antigen, GalNAcβ4-disialyl-Lc4; SDS-PAGE, sodium dodecyl sulfate polyacrylamide gel electrophoresis; SLe^a, sialyl-Lewis^a; SLe^x, sialyl-Lewis^x.

Grant sponsors: Biotechnology and Biological Sciences Research Council (BBSRC), the Wellcome Trust; Grant sponsor: Research Councils UK Basic Technology; Grant number: GR/S79268; Grant sponsors: Malaysian Perdana Scholarship, Imperial College, Japan Science and Technology Agency (JST).

Tsutomu Fujimura, Yasuro Shinohara, Bérangère Tissot and Poh-Choo Pang contributed equally to this study.

***Correspondence to:** Division of Molecular Biosciences, Faculty of Natural Sciences, Imperial College London, London SW7 2AZ, United Kingdom or Laboratory of Advanced Chemical Biology, Graduate School of Advanced Life Science, Hokkaido University N21, W11, Kita-ku, Sapporo 001, Japan or Department of Pathobiology, University of Washington and Pacific Northwest Research Institute, 720 Broadway, Seattle, WA, USA or Department of Microbiology, University of Washington, and Pacific Northwest Research Institute 720 Broadway, Seattle, WA, USA.
E-mail: hakomori@u.washington.edu

Received 27 December 2006; Accepted after revision 7 May 2007
DOI 10.1002/ijc.22958
Published online 5 September 2007 in Wiley InterScience (www.interscience.wiley.com).

UICC Publication of the International Union Against Cancer
global cancer control

Material and methods

Materials

Anti-human haptoglobin rabbit antibodies were from Dako (Carpinteria, CA). Peroxidase-coupled goat anti-rabbit IgG, used as secondary antibody was from Santa Cruz Biotech (Santa Cruz, CA). Chemiluminescent detection system (Super Signal West Pico) was from Pierce Biotechnology (Rockford, IL).

General procedure: Steps for serum collection and haptoglobin analysis

Step 1. Sera from patients with prostate cancer, or benign prostate disease, were collected based on diagnosis of patients by biopsy with histological examination by expert clinical pathologist, at the Dept. of Urology, Tohoku University School of Medicine, and sent in frozen state to Pacific Northwest Research Institute (PNRI), Seattle, WA, USA. The Ethics Committees of both Tohoku University and PNRI approved the study. PSA values of sera were also recorded (see below). PSA value (ng/ml) is given in parenthesis after case number.

a. Sera from prostate cancer. Case 5 (48.7); Case 21 (7.2); Case 23 (12.8); Case 32 (3.9); Case 40 (5.8); Case 71 (5.6); Case 72 (5.2); Case 76 (2.0).
b. Sera from benign prostate disease: Case 6 (7.3); Case 33 (3.0); Case 43 (9.2); Case 77 (13.2); Case 92 (3.9); Case 105 (13.6); Case 137 (4.1); Case 150 (6.6).

Serum volume sent from Tohoku University was 0.5–1.0 ml for each case. Sera from 8 cases each of prostate cancer and benign prostate disease were respectively combined and used for preparation of haptoglobin β-chain and α2-chain followed by examination of *N*- and *O*-glycosylation status. Sera from 8 normal subjects (volunteer workers) were prepared at PNRI.

Step 2. Combined sera as above containing equal protein quantity, or sera from normal subjects, were used for (*i*) determination of level of haptoglobin β-chain and α2-chain by Western blot analysis followed by densitometry of each band; (*ii*) affinity separation of haptoglobin by hemoglobin conjugated to Sepharose column; (*iii*) separation and purification of β-chain and α-chain, after cleavage of disulfide bonds by reductive alkylation. Procedures (*i*), (*ii*) and (*iii*) were performed at PNRI, Seattle, WA. Purified haptoglobin β-chain was sent to both Laboratory of Advanced Chemical Biology, Hokkaido University, Japan, and to Division of Molecular Biosciences, Imperial College London, UK.

Step 3. (*i*) Separation of tryptic glycopeptide-1, -2 and -3, covering each *N*-glycosylation site of haptoglobin β-chain, and determination of their structures, and (*ii*) determination of N-linked glycan structure released from each tryptic glycopeptide by PNGase-F (Roche Applied Science), were performed by the Hokkaido University group. (*iii*) In addition, total N-linked glycan of purified haptoglobin β-chain released by PNGase-F directly applied on haptoglobin β-chain, with particular focus on structure of fucosylation at antenna, was performed by the Imperial College London group.

Step 4. Structures of O-linked glycans from purified haptoglobin released by reductive β-elimination, and presence or absence of any known glycosyl epitope such as RM2 epitope, were rigorously studied by the Imperial College London group.

Serum haptoglobin levels

Step 2-(i). Individual sera (12 from prostate cancer cases, 9 each from benign prostate disease and from normal subjects) were used for determination of haptoglobin levels. An aliquot of serum containing equal 0.25-μg protein from each case was subjected to Western blot with anti-human haptoglobin rabbit antibodies, followed by secondary goat anti-rabbit IgG, and finally chemiluminescent detection system, as described previously.[20] The protein level of each serum sample was determined using a Micro-BCA protein assay reagent kit (Pierce).

Intensities of bands for β-chain and α2-chain from normal subjects, benign prostate disease, and prostate cancer were determined by densitometry with Scion Image program, as described in the Figure 1*a* legend.

Purification of haptoglobin and separation of β-, α2- and α1-chains

Step 2-(ii). Preparation of human serum haptoglobin by hemoglobin-affinity column. Human serum haptoglobin was prepared by affinity chromatography using freshly prepared human hemoglobin conjugated to Sepharose 4B, by the cyanogen bromide activation method as described previously.[21] Combined sera (~2–3 ml) were subjected to hemoglobin-Sepharose 4B column (1.0 × 18 cm^2, volume 14 ml) prepared in PBS (-) medium, pH 7.2 (see Abbreviations). An LKB peristaltic pump was used, and the flow rate was 0.5 ml/min. The eluent was monitored at 280 nm using a Waters 484 Tunable absorbance detector. A Gilson fraction collector model 203 was used, and 5-ml fractions were collected.

Applying human serum on the hemoglobin affinity column, most of the serum proteins passed through with PBS (-) wash, which was followed by washing with 0.15 M NaCl, pH 11 to elute apo AI. Finally, haptoglobin was eluted with 5 M urea in 0.15 M NaCl pH 11 solution. The eluate for haptoglobin was desalted and concentrated with an Amicon Centricon Plus-70 (Millipore) using Beckman centrifuge model J-6M at 3,000*g* for 10 min. The concentrated solution was diluted several times with 30-ml pure water, reconcentrated to remove urea, and finally lyophilized. Total haptoglobin fraction from ~2–3 ml serum, adsorbed on and eluted from hemoglobin column as above, was ~200–250 μg.

Step 2-(iii). Separation of haptoglobin β-, α2- and α1-chains by reductive alkylation followed by gel filtration. Haptoglobin purified as above is a hetero-tetramer cross-linked with inter and intra S–S bridges $(\alpha\beta)_2$. The subunits were separated by reductive alkylation with acrylamide as described previously.[20,22] Briefly, crude haptoglobin (~200 μg) was dissolved in 100 mM NH_4HCO_3, pH 8.5, and mixed with a vortex. Dithioerythritol was added to a final concentration of 150 mM and the pH was adjusted to 8.3 using 1 N NaOH before incubation at 37°C for 1 hr under nitrogen to cleave the S–S cross-links. Alkylation of the thiol groups was performed with 300 mM acrylamide to form propionamide cysteine (PAM) derivatives. The alkylation reaction was stopped on ice and the mixture was filtered with Millipore Ultrafree-MC (0.45 μm).

Separation of alkylated haptoglobin β-, α2- and α1-chains was performed by gel filtration through Superdex200™ 10-300GL (1.0 × 30 cm^2, bed volume 24 ml), in 50 mM phosphate buffer, pH 7.4, containing 0.15 M NaCl (PBS (-)). The HPLC (Waters 490) column was attached to a Waters UV detector and a Gilson fraction collector (model 203) was used. The flow rate was 0.4 ml/min. Each subunit was collected as 1 fraction and dialyzed using Spectra/Por molecular porous membrane tubing (MWCO 3.500, diameter 34 mm) (Spectrum Laboratories, Rancho Dominguez, CA) against 0.1% acetic acid for 40–50 hr. The solution was then transferred to an Eppendorf tube (1.5 ml) and lyophilized.

N-linked and O-linked carbohydrate analysis by mass spectrometry

Step 3-(i). Separation of tryptic glycopeptide-1, -2 and -3, covering each N-glycosylation site of haptoglobin β-chain, and determination of their structures by MALDI-TOF MS. Purified haptoglobin β-chain (~2 μg) from prostate cancer, benign prostate disease and normal subjects, respectively, was subjected to quantitative *N*-glycan profiling analysis, at the Laboratory of Advanced Chemical Biology, Hokkaido University. Each haptoglobin β-chain was reductively alkylated and digested with

trypsin, and *N*-glycans were enzymatically liberated from each haptoglobin β-chain using PNGase-F, and purified by a combination of methods previously described, with some modifications.[23–25] The sialic acid residue(s) of the *N*-glycans were methylesterified,[26] and labeled with aoWR.[27] For analyses of glycopeptides having N-linked glycan, purified haptoglobin β-chain (4–8 μg) was dried by centrifuge concentrator (Speed-Vac, Savant), and solubilized with 50 mM ammonium bicarbonate (pH 7.8) at a concentration of 0.2–0.4 mg/ml. Samples were digested with 0.5 μg modified trypsin at 37°C for 2 hr. The reaction was terminated by heating at 100°C for 3 min. The tryptic glycopeptides (glycopeptide-1, -2 and -3; see Results) derived from haptoglobin β-chain were purified with hydrophilic affinity isolation and reverse phase HPLC technique as described previously.[28] Briefly, the tryptic digest was mixed with a 15-μl packed volume of Sepharose 4B in 1 ml of an organic solvent of 1-butanol/ethanol/H_2O (4:1:1, v/v). After gentle shaking for 45 min, the gel was washed twice with the organic solvent, and then incubated with an aqueous solvent of ethanol/H_2O (1:1, v/v) for 30 min. The solution phase was recovered, dried and further fractionated by HPLC on a C18 column with a linear grandient elution of acetonitrile (5–50%, v/v) in 0.1% (v/v) trifluoroacetic acid. The glycopeptide fractions were mixed with 2,5-dihydroxybenzoic acid (10 mg/ml in water) and subjected to linear TOF measurements using an Ultraflex TOF mass spectrometer equipped with pulsed ion extraction system (Bruker Daltonik GmbH, Bremen, Germany). The ions generated by a pulsed UV laser beam (nitrogen laser, 337 nm, 10 Hz) were accelerated to a kinetic energy of 25.0 kV.

Step 3-(ii). MS and MS/MS analysis of permethylated N- and O-glycans from prostate cancer haptoglobin. A sample of prostate cancer haptoglobin (20 μg) was reduced for 1 hr at 37°C in 50 mM Tris-HCl buffer (pH 8.5) containing a 4-fold excess of dithiothreitol and carboxymethylated with a 2-fold molar excess of iodoacetic acid for 1 hr at room temperature in the dark. Following dialysis at 4°C for 72 hr against 4 × 4.5 l of cold 50 mM ammonium bicarbonate, pH 7.5, and lyophilization, the sample was digested with sequencing-grade trypsin (Promega) (1 μg in 50 mM ammonium bicarbonate, pH 8.5, for 18 hr at 37°C). The reaction was stopped by adding a few drops of acetic acid to the solution. The sample was lyophilized, dissolved in 150 μl (5% (v/v)) acetic acid, and purified using a SepPak cartridge C_{18} (Waters), as described.[29] The purified glycopeptides were digested with PNGase-F in 50 mM ammonium bicarbonate (pH 8.5) containing 10 U of enzyme at 37°C over 18 hr. The sample was lyophilized, and the released *N*-glycans were purified using a SepPak cartridge C_{18} (Waters Corp.). Permethylation and sample clean-up were performed using the sodium hydroxide protocol, as described previously.[29]

Steps 3-(iii) and -(iv). For *O*-glycan analysis, fractions from the gel filtration column corresponding to the α2- and β-chains (see above and Fig. 1*c*) were subjected to reductive elimination by adding 400 ml of 1 M potassium borohydride (dissolved in 0.1 M potassium hydroxide) for 24-hr incubation at 45°C. The reaction was stopped by adding a few drops of acetic acid. Further cleaning of the removed glycans was achieved by Dowex beads minicolumn purification followed by borate removal using 10% of methanolic acetic acid.[29] Permethylation and sample clean-up were performed using the sodium hydroxide protocol, as described previously.[29]

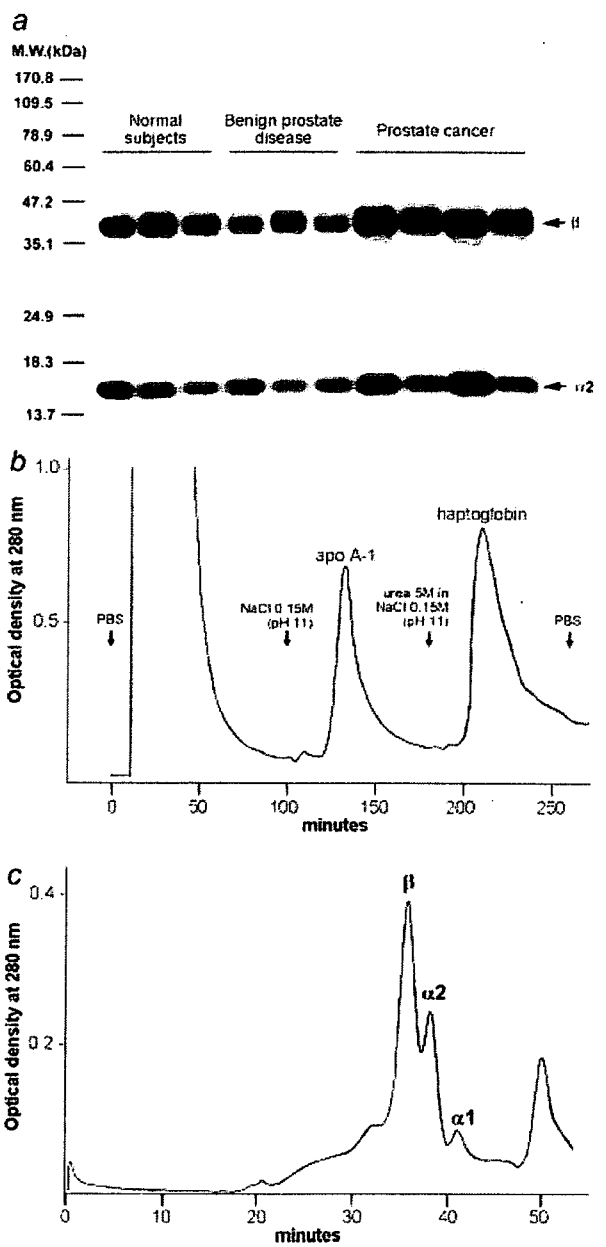

FIGURE 1 – Pattern of serum haptoglobin, affinity purification, and separation of β-, α1- and α2-chains. (*a*) Pattern of haptoglobin β-chain and α2-chain separated by 1-D SDS-PAGE, with Western blot with anti-haptoglobin antibodies. In total, 9 cases of normal subjects, 9 cases of benign prostate disease, and 12 cases of prostate cancer were analyzed. The figure shows 3 cases of normal subjects, 3 cases of benign prostate disease, and 4 cases of prostate cancer. For summary of analysis, see Table I. 0.25-μg protein from each serum was separated on 1-D SDS-PAGE, as described previously.[20] Proteins on a gel were blotted onto Immobilon P using a tank type apparatus from Nihon Eido (Tokyo, Japan) at 45 V for 50 min, in trans-blot buffer containing 10 mM CAPS and 10% methanol at pH 11. The membranes were blocked with 5% skim milk for 2 hr and incubated overnight with primary anti-human haptoglobin rabbit antibody (Dako). Peroxidase-coupled goat anti-rabbit IgG was used as secondary antibody. Finally, chemiluminescent detection system (Super Signal West Pico, Pierce Biotechnology) was used to enhance the bands or spots stained. (*b*) Affinity chromatography of haptoglobin from sera of prostate cancer patients. About 5 ml of serum from prostate cancer patients was loaded on hemoglobin-Sepharose 4B affinity column. (*c*) Separation of haptoglobin β-, α1- and α2-chains by gel filtration through Superdex200™ 10-300GL column. Crude haptoglobin (~200 μg) was reduced with dithioerythritol and alkylated with acrylamide. Experimental conditions for *b* and *c*: see Material and methods.

TABLE I – DENSITOMETRIC DETERMINATION OF WESTERN BLOTTED BANDS OF HAPTOGLOBIN β-AND α2-CHAINS BY ANTI-HAPTOGLOBIN ANTIBODIES IN 9 CASES EACH OF NORMAL SUBJECTS AND BENIGN PROSTATE DISEASE, AND 12 CASES OF PROSTATE CANCER

	n	mean ± SD	Significance of difference
β-chain			
Normal	9	8049 ± 2063	$p < 0.01$
Benign prostate	9	6866 ± 1647	
Prostate cancer	12	13462 ± 1487	
α2-chain			
Normal	9	8108 ± 2767	$p < 0.01$
Benign prostate	9	7673 ±1825	
Prostate cancer	12	13084 ± 3064	

MALDI-TOF MS data on permethylated samples were acquired at Imperial College London using a Perseptive Biosystems Voyager DE-STR™ mass spectrometer in the reflector mode with delayed extraction. MS/MS data were acquired using a 4800 MALDI-TOF/TOF (Applied Biosystems) mass spectrometer. The collision energy was set to 1 kV, and argon was used as collision gas. Samples were dissolved in 10 µl methanol and mixed at a 1:1 ratio (v/v) with 2,5-dihydrobenzoic acid as matrix.

Results

Haptoglobin levels in sera of prostate cancer patients, benign prostate disease and normal subjects

Haptoglobin levels in sera of prostate cancer patients were significantly higher than those from benign prostate disease or normal subjects, as determined by Western blot analysis of both β- and α2-chain with anti-haptoglobin antibodies (Fig. 1*a*). Mean densitometric values for 12 cases of prostate cancer, compared to 9 cases of benign prostate disease, and 9 normal subjects, for β-chain, were 1.9 and 1.7 times higher, respectively. Values for the α2-chain were 1.7 and 1.6 times higher, respectively. Each of these differences was statistically significant ($p < 0.01$), as indicated (Table I).

Separation of haptoglobin into its β-, α2- and α1-chains

To search for cancer-associated glycosyl epitopes in haptoglobin we chose to isolate its subunits and search for glycopeptides after tryptic digestion.

Thus haptoglobin from sera of prostate cancer patients, benign prostate disease, or normal subjects was affinity purified on a hemoglobin-Sepharose 4B column and the β-, α2- and α1-chains were separated after reductive alkylation, as detailed in Material and methods. A typical example of the affinity chromatography pattern is shown in Figure 1*b*, and a typical example of the gel filtration pattern of the β-, α2- and α1-chains is shown in Figure 1*c*. Once again, we could observe that the quantities of the β- and α2-chain in prostate cancer patients were significantly higher than those in benign prostate disease or normal subjects (Table I).

Glycomics profiling of the β-chain reveals enhanced fucosylation in prostate cancer

A similar quantity of purified haptoglobin β-chain (*e.g.*, ~2 µg per analysis) from prostate cancer, benign prostate disease and normal subjects was subjected to PNGase-F digestion. The released N-linked glycans were purified from a crude digestion mixture by glycoblotting technique through reaction of the reducing end of the carbohydrate with an amino-oxime group or hydrazide group affixed on solid phase.[23] To perform quantitative MALDI-TOF analysis with high sensitivity, the captured glycans were further methylesterified at the carboxyl group of sialic acid residue(s),[26] and were derivatized with aoWR.[27]

Spectra of the N-linked glycans obtained from the β-chain of prostate cancer, benign prostate disease and normal subjects are shown in Figure 2. As shown in the annotations, the major glycans shared by all 3 samples are mono- and disialylated bi-antennary

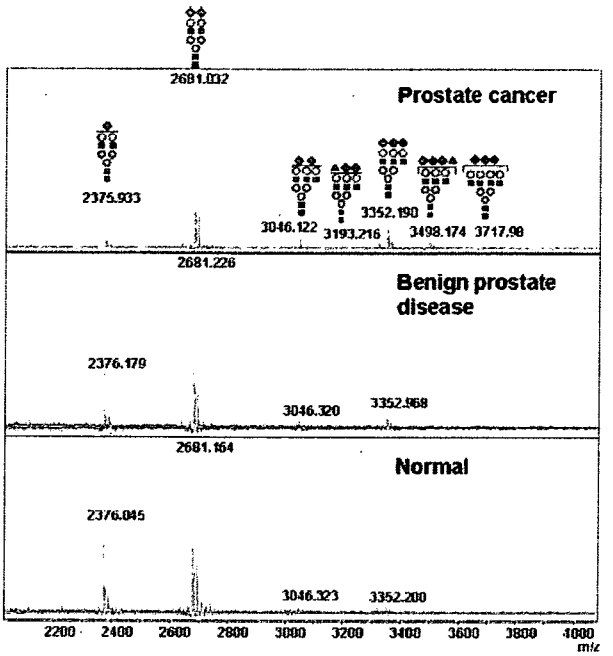

FIGURE 2 – MALDI-TOF spectra showing differences in N-linked glycans of haptoglobin β-chain from sera of prostate cancer, benign prostate disease, and normal subjects. Glycans were released by PNGase-F, methylesterified at the carboxyl group of sialic acid(s), and derivatized with aoWR. Keys are given in the box and correspond to Consortium for Functional Glycomics symbols (http://www.functionalglycomics.org/fg/). [Color figure can be viewed in the online issue, which is available at www.interscience.wiley.com.]

structures (theoretical *m/z* 2,375.9 and 2,681.0). All 3 samples also contain a minor trisialylated tri-antennary glycan, the molecular ion at *m/z* 3,352.2 and 3,352.9, which is much more abundant in prostate cancer than in benign prostate disease or normal subjects. A tiny amount of disialylated tri-antennary glycan, the molecular ion at *m/z* 3,046.2, is observed in the prostate cancer and benign prostate disease samples. The most striking difference between the samples is the presence of *m/z* 3,498.2 in the prostate cancer spectrum (Fig. 2, upper panel). This signal, which is absent in the spectra from benign prostate disease and normal subjects (Fig. 2, middle and bottom panels), corresponds to a mono-fucosylated tri-antennary glycan, the molecular ion at *m/z* 3,498.2.

Fucosylated tri-antennary N-glycans are specific to one of the glycosylation domains of the β-chain

The consensus sites for *N*-glycosylation are Asn-184 (N184), N207, N211 and N241. To investigate the location of the fucosylated *N*-glycans observed in the glycomic profiling, the β-chain samples from prostate cancer, benign prostate disease, and normal subjects were subjected to tryptic digestion and MALDI analysis. Tryptic digestion was predicted to yield 3 glycopeptides: (*i*) 203-215 carrying 2 glycosylation sites, N207 and N211, (*ii*) 236-251 carrying 1 glycosylation site at position N241 and (*iii*) 179-202 carrying 1 glycosylation site at position N184. The resulting glycopeptides were fractionated by successive hydrophilic affinity isolation and reversed-phase HPLC, and were analyzed by MALDI-TOF mass spectrometry. Each glycopeptide yielded a cluster of molecular ions because of glycan heterogeneity. Under the chromatographic conditions employed, we observed that glycopeptides of different glycoforms on the same peptide tended to elute in close proximity on reversed-phase chromatography analyses. The relative microheterogeneity of different glycoforms present at a particular *N*-glycosylation site(s) was determined by com-

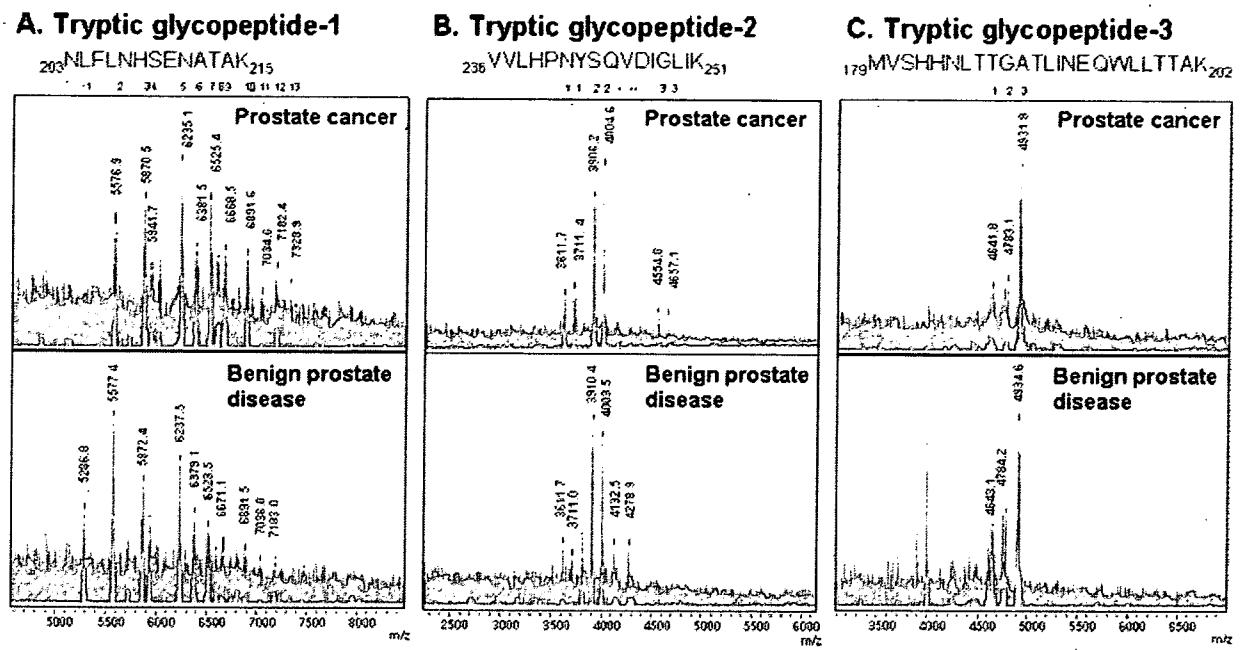

FIGURE 3 – Variation in N-linked glycan structures in tryptic glycopeptides from haptoglobin β-chain. MALDI-TOF spectra of "tryptic glycopeptide-1" (including N-linked glycans present at N207 and N211), "tryptic glycopeptide-2" (including N-linked glycans present at N241), and "tryptic glycopeptide-3" (including N-linked glycans present at N184) are shown in *a*, *b* and *c*, respectively. Upper panels: haptoglobin β-chain of sera from prostate cancer patients. Lower panels: haptoglobin β-chain of sera from benign prostate disease. [Color figure can be viewed in the online issue, which is available at www.interscience.wiley.com.]

paring the signal intensities upon mixing equivalent volumes from each successive fraction containing the same peptide backbone.

Elucidation of the microheterogeneity of peptide that contains N207 and N211 (glycopeptide-1) revealed that structures of N-linked glycans and their quantity from β-chain of prostate cancer *vs.* benign prostate disease differed substantially. Prostate cancer (Fig. 3*a*, upper panel) exhibited notable increase in abundance of glycopeptides containing at least 1 tri-antennary glycan with fucosylated species. In benign prostate disease (Fig. 3*a*, lower panel), signals consistent with glycopeptides carrying triantennary glycans are significantly reduced in abundance compared with the prostate cancer sample.

The microheterogeneity of tryptic glycopeptide-2 and -3 (which contains N241 and N184, respectively) was elucidated in a similar fashion. Unfortunately, it was not possible to determine the glycosylation profiles of glycopeptides of normal subjects, due to limited sample availability. Differences in structure and quantity of prostate cancer *vs.* benign prostate disease are shown in Fig. 3*b*. Tri-antennary structure was found in prostate cancer, but not in benign prostate disease, at N241 in "tryptic glycopeptide-2." No tri-antennary structure was found in either prostate cancer or benign prostate disease at N184 in "tryptic glycopeptide-3" (Table II). From these analyses, it was found that only tryptic glycopeptide-1 gave signals consistent with fucosylated tri-antennary structures. Such marked differences in glycosylation at each *N*-glycosylation site were revealed for the first time.

Glycan structures attributable to each of the molecular ions are summarized in Table II. Sequences were assigned taking into account *m/z* values and the glycomics information arising from the MALDI profiling described earlier. The fucosylated components at *m/z* 6,638 and 7,328 are barely visible, indicating that glycopeptides carrying fucosylated glycans are also reduced as compared with the prostate cancer sample. The normal sample shows no convincing signals for fucosylated tri-antennary structures (data not shown). These findings are all consistent with the glycomics profile shown in Figure 2.

MS/MS analysis of permethylated derivatives reveals the location of fucosylation in prostate cancer N*-glycans and the absence of disialylated epitopes*

As described above, the analysis of the glycopeptides from control, benign and prostate cancer haptoglobin showed clear differences in the *N*-glycan repertoire, notably the presence of significant quantities of sialylated and fucosylated tri-antennary structures. However, the methods used provided no information on the location of the fucose, and were not optimal for detection of very minor components which might carry RM2-related structures.[16] To explore these issues, further study was performed by permethylation analysis, a powerful technique often used for structural elucidation of oligosaccharides. The major signals in the MALDI-TOF profile of a permethylated prostate cancer sample (Fig. 4) correspond to those observed in the initial glycomics analysis (Fig. 2). However, due to the analytical methods employed, many more minor components are observed, including a fucosylated bi-antennary structure (*m/z* 2,967), a difucosylated tri-antennary structure (*m/z* 3,952), and tetra-antennary structures (*m/z* 3,691; 3,865; 4,053; 4,226; 4,414; 4,587 and 4,762). The sequences shown in the annotations on Figure 4 were assigned using compositional information derived from *m/z* values and, where available, MS/MS data from MALDI-TOF/TOF analyses. Key data from the latter experiments are shown in Figure 5. To establish whether fucose is found on the core or the antenna of mono-fucosylated glycans, the molecular ions at *m/z* 2,967 and 3,778 were subjected to collisional activation in MS/MS experiments. The resulting data (Figs. 5*a* and 5*b*) show unequivocally that the majority of the fucosylation is on the antenna. Thus a good quality signal is observed at *m/z* 1,021 in both spectra corresponding to a SLe^x or SLe^a epitope (see inserts in Figs. 5*a* and 5*b*). In addition, abundant ions are present at high mass, corresponding to loss of this struc-

TABLE II – PUTATIVE GLYCAN STRUCTURES FROM HAPTOGLOBIN β-CHAIN, *m/z* VALUES, AND RELATIVE ABUNDANCE
[COLOR TABLE CAN BE VIEWED IN THE ONLINE ISSUE, WHICH IS AVAILABLE AT WWW.INTERSCIENCE.WILEY.COM.]

Peak No	m/z	Glycan structure			Relative abundance		
					Prostate cancer	Benign prostate	Normal subject
A: NLFLNHSENATAK(203-215)[1]							
1	5286.8 ± 9.0	[NeuAc1Hex2HexNAc2+Man3GlcNAc2] + [NeuAc1Hex2HexNAc2+Man3GlcNAc2)]	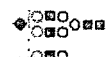	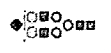	ND	9.6	17.8
2	5576.9 ± 15.0	[NeuAc1Hex2HexNAc2+Man3GlcNAc2)] + [NeuAc2Hex2HexNAc2+Man3GlcNAc2]	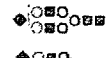	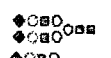	10.5	22.3	31.1
3	5870.5 ± 17.0	[NeuAc2Hex2HexNAc2+Man3GlcNAc2] + [NeuAc2Hex2HexNAc2+Man3GlcNAc2)]	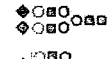	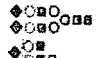	12.8	14.3	12.5
4	5941.7 ± 18.0	[NeuAc1Hex2HexNAc2+Man3GlcNAc2] + [NeuAc2Hex3HexNAc3+Man3GlcNAc2]		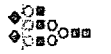	4.3	7.3	11.0
5	6235.1 ± 18.0	[NeuAc1Hex2HexNAc2+Man3GlcNAc2] + [NeuAc3Hex3HexNAc3+Man3GlcNAc2]	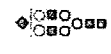	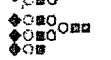	17.0	17.0	9.2
		[NeuAc2Hex2HexNAc2+Man3GlcNAc2)] + [NeuAc2Hex3HexNAc3+Man3GlcNAc2]		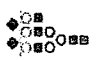			
6	6381.5 ± 18.0	[NeuAc1Hex2HexNAc2+Man3GlcNAc2] + [NeuAc3Hex3HexNAc3+Man3GlcNAc2 +Fuc]		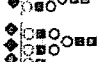	6.7	8.2	5.8
7	6525.4 ± 18.0	[NeuAc2Hex2HexNAc2+Man3GlcNAc2] + [NeuAc3Hex3HexNAc3+Man3GlcNAc2)]			14.7	6.4	6.0
8	6597.3 ± 17.0	[NeuAc2Hex3HexNAc3+Man3GlcNAc2] + [NeuAc2Hex3HexNAc3+Man3GlcNAc2]		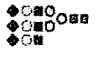	4.4	3.3	6.6
9	6668.2 ± 18.0	[NeuAc2Hex3HexNAc3+Man3GlcNAc2] + [NeuAc2Hex3HexNAc3+Man3GlcNAc2 + Fuc]			7.3	4.1	ND
10	6891.6 ± 18.0	[NeuAc2Hex3HexNAc3+Man3GlcNAc2)] + [NeuAc3Hex3HexNAc3+Man3GlcNAc2]			7.3	3.4	ND
11	7034.6 ± 17.0	[NeuAc2Hex3HexNAc3+Man3GlcNAc2] + [NeuAc3Hex3HexNAc3+Man3GlcNAc2 + Fuc]		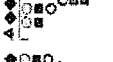	4.5	4.1	ND
12	7182.4 ± 20.0	[NeuAc3Hex3HexNAc3+Man3GlcNAc2] + [NeuAc3Hex3HexNAc3+Man3GlcNAc2]		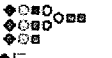	6.3	ND	ND
13	7328.9 ± 20.0	[NeuAc3Hex3HexNAc3+Man3GlcNAc2] + [NeuAc3Hex3HexNAc3+Man3GlcNAc2 + Fuc]			4.2	ND	ND
					100.0	100.0	100.0
B. VVLHPNYSQVDIGLIK (236-251)[2]							
1′	3611.7 ± 9.0	[NeuAc1Hex2HexNAc2+Man3GlcNAc2] - 98 (N-terminal Val residue?)	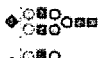		8.8	11.2	ND
1	3711.4 ± 9.0	[NeuAc1Hex2HexNAc2+Man3GlcNAc2]			10.6	8.0	ND
2′	3906.2 ± 9.0	[NeuAc2Hex2HexNAc2+Man3GlcNAc2] - 98 (N-terminal Val residue?)	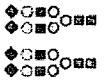		28.4	25.9	ND
2	4004.6 ± 9.0	[NeuAc2Hex2HexNAc2+Man3GlcNAc2]	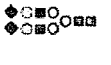		35.5	30.0	ND
2*	4132.5 ± 15.0	[NeuAc2Hex2HexNAc2+Man3GlcNAc2] +128			4.5	11.6	ND
2**	4278.9 ± 15.0	[NeuAc2Hex2HexNAc2+Man3GlcNAc2] +128 + 146 (Fuc?)			2.1	8.6	ND
3′	4554.8 ±18.0	[NeuAc3Hex3HexNAc3+Man3GlcNAc2] - 102 (N-terminal Val residue?)			5.5	4.7	ND
3	4657.1 ± 18.0	[NeuAc3Hex3HexNAc3+Man3GlcNAc2]			4.6	ND	ND
					100.0	100.0	
C: MVSHHNLTTGATLINEQWLLTTAK(179-202)[3]							
1	4641.8 ± 9.0	[NeuAc1Hex2HexNAc2+Man3GlcNAc2)]			14.2	16.5	ND
2	4783.1 ± 15.0	[NeuAc1Hex2HexNAc2+Man3GlcNAc2 + Fuc]			21.1	27.5	ND
3	4931.9 ± 17.0	[NeuAc2Hex2HexNAc2+Man3GlcNAc2]			64.7	56.0	ND
					100	100	

ND: not determined, due to limited sample availability.
[1]N-207 & 211, MW1458.735.–[2]N-241, MW1795.0112.–[3]N-184, MW2679.3923.

ture from the respective molecular ions (*m/z* 1,969 and *m/z* 2,780 in Figs. 5*a* and 5*b*, respectively). Similar analysis of the difucosylated tri-antennary glycan at *m/z* 3,952 showed that this glycan predominantly carries 2 SLe^x or SLe^a antennae (Fig. 5*c*). No signals were observed consistent with alternative fucosylation of any of these glycans, although we cannot rule out minor core fucosylation because there are relatively high levels of background noise in the vicinity of the *m/z* values corresponding to loss of the reducing end sugar (for example, *m/z* 2,690 and 3,501 in Figs. 5*a* and 5*b*, respectively).

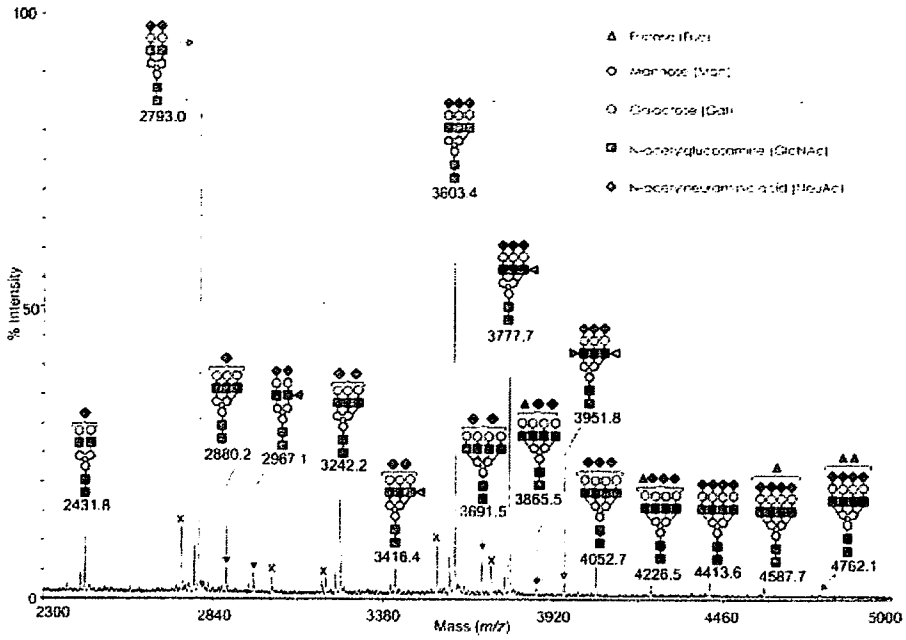

FIGURE 4 – MALDI-TOF spectra of prostate cancer haptoglobin *N*-glycans. Glycans were released by PNGase-F, permethylated, and subjected to Sep-Pak cleanup ("Material and methods"). Data from one of the fractions collected upon SepPak cleanup are shown. Cartoon assignments are based on the precise fit between composition calculations and the *m/z* ($z = 1$) ratio of the molecular ions detected. These cartoons represent the most likely structures taking into account the biosynthetic pathways and, when available, MALDI TOF/TOF MS/MS data. Each of the major peaks presents a minor peak distant by 14 mass units that corresponds to an under-methylated species. Ions labeled with a cross correspond to permethylation artifacts. [Color figure can be viewed in the online issue, which is available at www.interscience.wiley.com.]

To search for the possible presence of glycans containing RM2-related epitopes,[16] we calculated *m/z* values for bi- and tri-antennary glycans carrying 1 or more RM2 sequences and/or its disialylated sub-structure (Table III). None of these *m/z* values was found to be more abundant than the background noise. We know from other studies in our laboratory that minor molecular ions which are hidden in the background are frequently observed in MS/MS experiments because of lower background noise. Therefore, we selected each of the calculated *m/z* values in Table III for MS/MS analysis, together with observed molecular ions at similar masses, which served as controls for sensitivity of detection of fragment ions. Excellent MS/MS data were obtained on all the visible molecular ions in the vicinity of the calculated *m/z* values, *i.e.*, from *m/z* 3,100 up to *m/z* 4,200, and these components are annotated in Figure 4. In contrast, no fragment ions consistent with sialylated glycans were obtained when any of the calculated *m/z* values given in Table III were selected.

Reductive elimination experiments reveal some O-glycosylation in prostate cancer haptoglobin

Having failed to detect the RM2 structure on the *N*-glycans of haptoglobin, we investigated the possibility that haptoglobin might be *O*-glycosylated, and that the RM2 epitope might be associated with this class of glycans. Although *O*-glycans have not previously been found in haptoglobin, NetOGlyc (http://www.cbs.etu.dk/services/NetOGlyc/) analysis of the haptoglobin sequence indicates that some sites in both the β- and α-chains are favorable for *O*-glycosylation. To search for putative *O*-glycans, the gel-purified β- and α2-chains of prostate cancer haptoglobin (Fig. 1*c*) were subjected to reductive elimination followed by permethylation and MS analysis. Reductive elimination is known to efficiently release *O*-glycans from glycoproteins, and this treatment also partially releases *N*-glycans. Thus, the presence and the abundance of *N*-glycans in the resulting mass spectra serve as a control for the efficiency of the reaction.

Figuer 6 shows the MALDI-MS profile obtained for the purified β-chain. In the total spectrum (Fig. 6*a*), the 2 major *N*-glycan structures are annotated. The *m/z* region corresponding to molecular ions consistent with *O*-glycan structures have been magnified (Fig. 6*b*). Two molecular ions corresponding to sialylated core Type 1 *O*-glycans have been assigned (*m/z* 895 and 1,256). However, the high background in the vicinity of these 2 ions, and their low abundance, prevent their unequivocal identification. Therefore, these ions were subjected to MS/MS analysis. For both ions, characteristic fragment ions consistent with the loss of sialic acid residues (*m/z* 520, and *m/z* 881 and 472) confirmed the presence of mono- and disialylated core Type 1 *O*-glycans (Figs. 7*a* and 7*b*, respectively). Very similar results were obtained from analysis of the purified α2-chain of prostate cancer haptoglobin (data not shown).

Having discovered that *O*-glycans are indeed present on prostate cancer haptoglobin, albeit at very low levels, we searched for RM2-related epitopes on this family of glycans. Following the same strategy as the 1 used for *N*-glycans, *m/z* values corresponding to predicted core Type 1 and core Type 2 *O*-glycan sequences carrying RM2 and di-sialylated epitopes were subjected to MS/MS analysis. No evidence for such structures was found using this methodology, despite excellent data being acquired for several very minor *N*-glycans of similar *m/z* values (data not shown).

Discussion

This study has addressed the following aspects of serum haptoglobin of patients with prostate cancer *vs.* benign prostate disease, and normal subjects: (*i*) changes of haptoglobin level; (*ii*) differences in *N*-glycosylation level and *N*-glycan structures; (*iii*) haptoglobin as a possible carrier of the RM2 epitope which was previ-

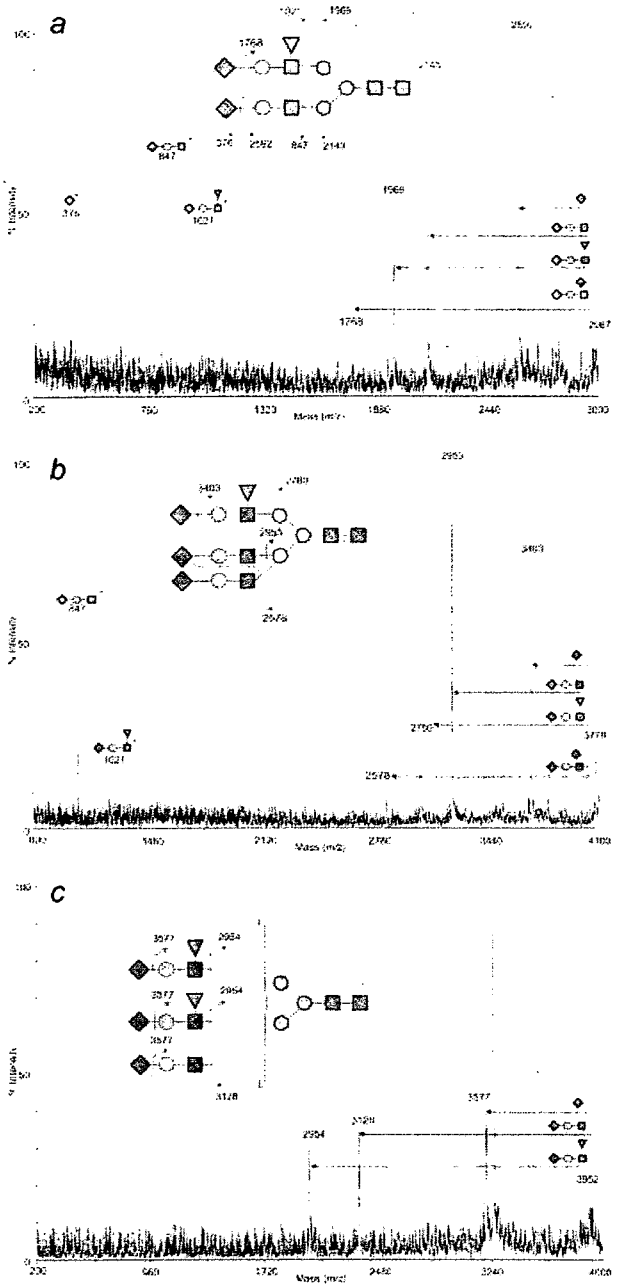

FIGURE 5 – MALDI-TOF/TOF MS/MS spectra of *m/z* 2,967 (*a*), *m/z* 3,778 (*b*) and *m/z* 3,952 (*c*) *N*-glycans from prostate cancer haptoglobin. In each of the 3 panels, the major component is shown in the schematic. Fucose residue(s) are located on the antennae as demonstrated by the presence of fragment ion at *m/z* 1,021 (*a* and *b*) and/or by the presence of an ion corresponding to the loss of this structure (*m/z* 2,954, *c*). For keys, see Figure 2 [Color figure can be viewed in the online issue, which is available at www.interscience.wiley.com.]

ously suggested to be enhanced specifically in prostate cancer; (*iv*) the possible presence of *O*-glycans.

The expression of haptoglobin was found to be significantly elevated in the sera of prostate cancer patients compared to benign prostate disease patients and normal subjects. This is consistent with many previous observations on increased levels of acute phase proteins such as haptoglobin in the sera of patients with inflammatory diseases and cancer.[19,30,31] This may be due to the epithelial-mesenchymal transition phenomenon. Furthermore, actively-growing tumor cells show many similar properties to inflammatory cells, particularly activated fibroblasts.[32,33]

Based on our structural studies of haptoglobin, we conclude the following: (*i*) Bi-antennary mono- and disialylated glycans are common to all samples and were the major structures observed at all *N*-glycosylation sites. Significantly, tri-antennary structures together with a few tetra-antennary structures were also found, particularly at N207 and N211, and their levels were higher in prostate cancer samples than in benign prostate disease or normal samples. (*ii*) Fucosylated glycans were most abundant in the prostate cancer sample. (*iii*) The fucoses were found to be mainly on the antenna(e) rather than the cores of the *N*-glycans. This was rigorously established by MALDI-TOF-TOF MS/MS analysis of permethylated glycans. (*iv*) No *N*-glycans carrying the RM2 epitope or its analogue were detected, despite careful searches using highly sensitive mass spectrometric methodologies available. (*v*) In an attempt to explain the RM2 cross-reactivity of prostate cancer haptoglobin, we investigated the possible presence of *O*-glycans, since the Cad epitope was proposed as O-linked,[34] and both Cad and disialyl-Le^c (FH9) epitope[9] have close homology with RM2. High sensitivity MS/MS analysis provided unambiguous evidence for low levels of *O*-glycosylation. This is the first observation that O-linked structures are present in haptoglobin. However, the glycans detected were mono- and disialylated core Type 1 structures, and no evidence was found for RM2 or analogous sequences such as Cad. In summary, despite extensive searches for the presence of RM2 and Cad sequences in the *N*- and *O*-glycans in haptoglobin, none was detected. Thus, the possible presence of RM2 epitopes in prostate cancer haptoglobin, as suggested through antibody staining studies (Saito et al., unpublished data), has not been confirmed by rigorous structural analysis, *i.e.*, glycosyl epitope originally assigned as GalNAcβ4-disialyl-Lc4 or its analogue is not detectable in haptoglobin. The specific structural attributes of prostate cancer haptoglobin that result in cross-reactivity with RM2 antibodies remain to be determined. It should be noted that mAbs (often IgM, less frequently IgG3) directed to disialyl glycosyl epitopes display "polyreactivity" with related or unrelated structures, surprisingly including actin, thyroglobulin, tubulin, DNA (particularly single-stranded).[35] mAb RM2 may react with unknown, non-carbohydrate structures associated with haptoglobin.

Over the past 20 years, many laboratories have investigated the levels and glycosylation patterns of serum haptoglobin from a range of cancers, including ovarian, breast, small cell lung, pancreatic and liver cancers, hoping to identify specific markers that might be suitable for diagnostic assays.[30,36–40] Over-expression of haptoglobin, and changes in the level of fucose and/or sialic acid residues, are common themes emerging from all these studies, but no cancer-specific glycoform of haptoglobin has been found to date. Our studies of prostate cancer haptoglobin have opened up 2 new avenues for investigation. First, the detection of *O*-glycans in haptoglobin is potentially an important observation because *O*-glycans have been identified as the major *in vivo* ligands for selectins. Moreover, there is evidence pointing to physiological regulation of *O*-glycosylation, notably in pregnancy.[41] It will be interesting, therefore, to characterize *O*-glycosylation of haptoglobin in ovarian and breast cancers. Second, our experiments have provided the first rigorous discrimination of core and antenna fucosylation in haptoglobin. Most of the previous studies employed lectins to probe changes in fucosylation, with consequent uncertainty in the precise fucosylation pattern. In those instances where more rigorous mass spectrometric methods were used, for example in the pancreatic cancer study,[40] the authors were unable to unambiguously establish the fucosylation sites in many of the glycans, particularly the multi-antennary components. Interestingly, in all previous studies where sites of fucosylation have been reported, increases in core fucosylation were observed, whereas antenna

TABLE III – POTENTIAL STRUCTURES FOR RM2 AND CAD EPITOPES
[COLOR TABLE CAN BE VIEWED IN THE ONLINE ISSUE, WHICH IS AVAILABLE AT WWW.INTERSCIENCE.WILEY.COM.]

Potential structures with RM2 epitope			Potential structures with Cad epitope		
m/z	Structures	Composition	*m/z*	Structures	Composition
3398		$Hex_5HexNAC_5NeuAc_3+Na^+$	3153		$Hex_5HexNAC_4NeuAc_3+Na^+$
4004		$Hex_5HexNAC_6NeuAc_4+Na^+$	3514		$Hex_5HexNAC_4NeuAc_4+Na^+$
4208		$Hex_6HexNAC_6NeuAc_4+Na^+$	3963		$Hex_6HexNAC_5NeuAc_4+Na^+$

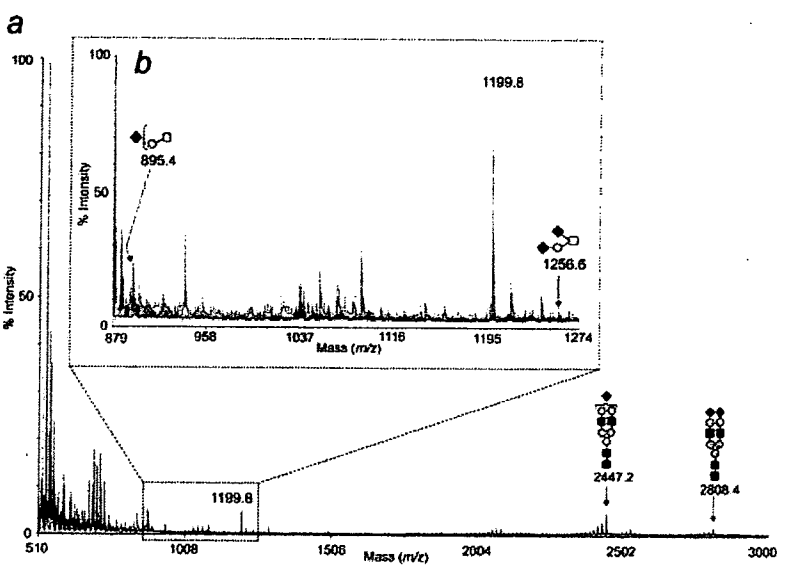

FIGURE 6 – MALDI-TOF spectrum of β-chain haptoglobin glycans released by reductive elimination. Purified β-chain from cancer prostate haptoglobin was subjected to reductive elimination. Glycans were subsequently permethylated, and subjected to Sep-Pak cleanup. See Figure 5 legend. (*a*) spectrum acquired from *m/z* 510 to *m/z* 3,000. (*b*) Magnified region comprised between *m/z* 879 to *m/z* 1,274, which has been expanded for clarity. For keys, see Figure 2. [Color figure can be viewed in the online issue, which is available at www.interscience.wiley.com.]

fucosylation was not always reported. In contrast, we observed significant levels of antenna fucosylation in prostate cancer haptoglobin, but core fucosylation was not detected. We suggest that quantitative comparisons of core versus antenna fucosylation of haptoglobin from different cancers might yield useful information for diagnostic purposes.

The presence of multi-antennary *N*-glycans (tri-antennary or more) is common not only in haptoglobin in prostate cancer (present study) and pancreas cancer,[40] but also in many other glycoproteins expressed in transformed cells. Compared to normal cells, transformed cells were found to express glycans with higher molecular mass.[42] Moreover, multi-antennary glycans were observed to be closely associated with oncogenic transformation[43,44] and have been suggested to be potential prognoses for cancer development and metastasis.[45]

Haptoglobin *N*-glycans from prostate cancer may be qualitatively different from those of benign prostate disease or normal subjects, if expression of multi-antennary N-linked structures with SLe^x / SLe^a at a defined site of haptoglobin β-chain is characteristic of prostate cancer. Therefore, combinations of antibodies directed to haptoglobin β-chain, *Phaseolus vulgaris*-L lectin (which reacts specifically with the β1-6GlcNAc branch common to tri- or tetra-antennary but not bi-antennary structure),[46,47] and antibodies directed to SLe^x/SLe^a, may provide diagnostic tools for prostate cancer.

Conversion of bi-antennary to multi-antennary structures, due to enhanced GlcNAc transferase-V, is generally accepted as a common phenotype, directly or indirectly controlled by oncogenes.[48–50] Expression of multi-antennary N-linked structures with modified fucosylation may be a common denominator in basic cancer-associated changes in haptoglobin. Further extensive glycomic studies will help clarify the relationship between glycosylation changes and disease progression in general.

Acknowledgements

A.D. is a BBSRC Professorial Fellow. B.T. was supported by a Research Councils UK Basic Technology Grant (GR/S79268). P.-C.P. was supported by a Malaysian Perdana Scholarship and by Imperial College.

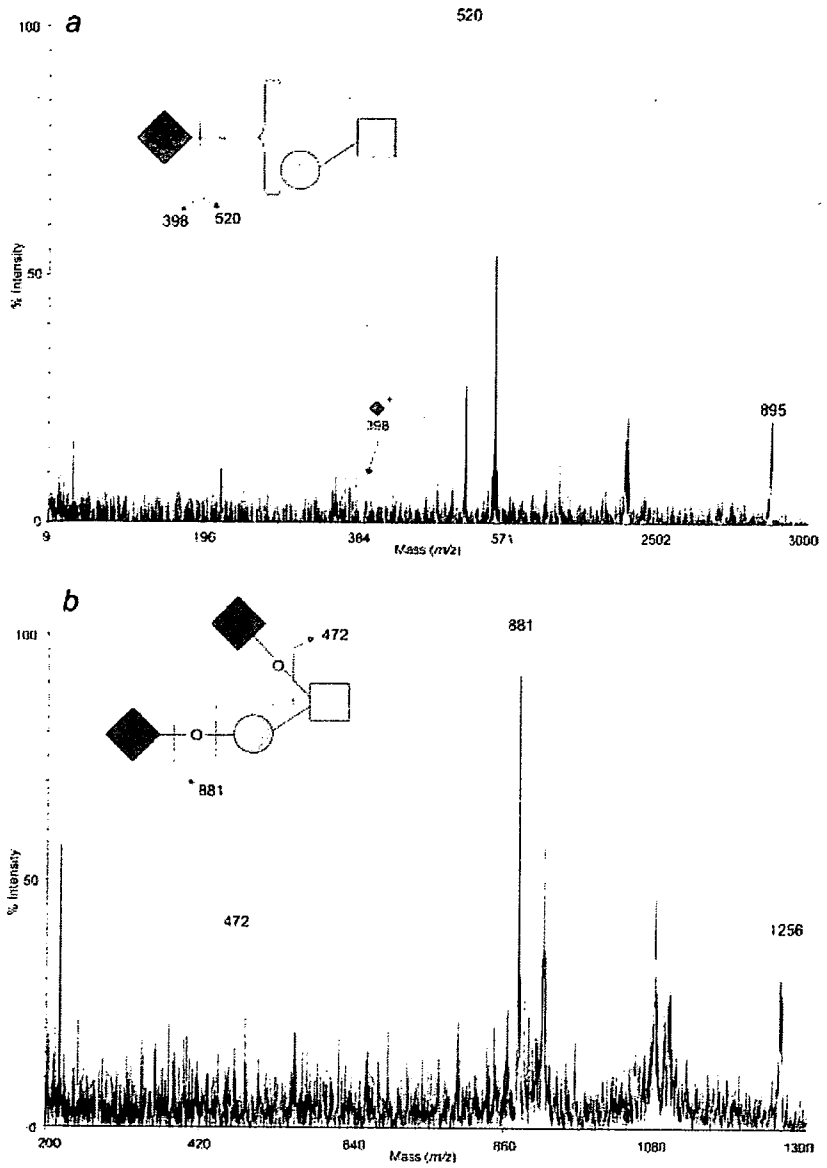

FIGURE 7 – MALDI-TOF/TOF MS/MS spectra of the signals at *m/z* 895 (*a*) and *m/z* 1,256 (*b*) in the Figure 6 spectrum. In each case a major fragment ion is observed corresponding to loss of sialic acid. For keys, see Figure 2. [Color figure can be viewed in the online issue, which is available at www.interscience.wiley.com.]

References

1. Hakomori S. Aberrant glycosylation in tumors and tumor-associated carbohydrate antigens. Adv Cancer Res 1989;52:257–331.
2. Livingston PO, Natoli EJ, Calves MJ, Stockert E, Oettgen HF, Old LJ. Vaccines containing purified GM2 ganglioside elicit GM2 antibodies in melanoma patients. Proc Natl Acad Sci USA 1987;84:2911–15.
3. Helling F, Shang A, Calves MJ, Zhang S, Ren S, Yu RK, Oettgen HF, Livingston PO. G_{D3} vaccines for melanoma: superior immunogenicity of keyhole limpet hemocyanin conjugate vaccines. Cancer Res 1994; 54:197–203.
4. Slovin SF, Ragupathi G, Adluri S, Ungers G, Terry K, Kim S, Spassova M, Bornmann WG, Fazzari M, Dantis L, Olkiewicz K, Lloyd KO, et al. Carbohydrate vaccines in cancer: immunogenicity of a fully synthetic globo H hexasaccharide conjugate in man. Proc Natl Acad Sci USA 1999;96:5710–15.
5. Hakomori S. Tumor-associated carbohydrate antigens defining tumor malignancy: basis for development of anti-cancer vaccines. Adv Exp Med Biol 2001;491:369–402.
6. Haglund C, Kuusela P, Jalanko H, Roberts PJ. Serum CA 50 as a tumor marker in pancreatic cancer: a comparison with CA 19-9. Int J Cancer 1987;39:477–81.
7. Hanisch FG, Uhlenbruck G, Peter-Katalinic J, Egge H. Structural studies on oncofetal carbohydrate antigens (Ca 19-9, Ca 50, and Ca 125) carried by O-linked sialyloligosaccharides on human amniotic mucins. Carbohydr Res 1988;178:29–47.
8. Magnani JL, Nilsson B, Brockhaus M, Zopf D, Steplewski Z, Koprowski H, Ginsburg V. A monoclonal antibody-defined antigen associated with gastrointestinal cancer is a ganglioside containing sialylated lacto-*N*-fucopentaose II. J Biol Chem 1982;257: 14365–9.
9. Fukushi Y, Nudelman ED, Levery SB, Higuchi T, Hakomori S. A novel disialoganglioside ($IV^3NeuAcIII^6NeuAcLc_4$) of human adenocarcinoma and the monoclonal antibody (FH9) defining this disialosyl structure. Biochemistry 1986;25:2859–66.
10. Stroud MR, Levery SB, Nudelman ED, Salyan MEK, Towell JA, Roberts CE, Watanabe M, Hakomori S. Extended type 1 chain glycosphingolipids: Dimeric Le^a ($III^4V^4Fuc_2Lc_6$) as human tumor-associated antigen. J Biol Chem 1991;266:8439–46.
11. Watanabe M, Ohishi T, Kuzuoka M, Nudelman ED, Stroud MR, Kubota T, Kodaira S, Abe O, Hirohashi S, Shimosato Y Hakomori S.

In vitro and *in vivo* antitumor effects of murine monoclonal antibody NCC-ST-421 reacting with dimeric Lea (Lea/Lea) epitope. Cancer Res 1991;51:2199–204.
12. Springer GF. T and Tn, general carcinoma autoantigens. Science 1984;224:1198–206.
13. Hirohashi S, Clausen H, Yamada T, Shimosato Y, Hakomori S. Blood group A cross-reacting epitope defined by monoclonal antibodies NCC-LU-35 and -81 expressed in cancer of blood group O or B individuals: its identification as Tn antigen. Proc Natl Acad Sci USA 1985;82:7039–43.
14. Kjeldsen TB, Clausen H, Hirohashi S, Ogawa T, Iijima H, Hakomori S. Preparation and characterization of monoclonal antibodies directed to the tumor-associated O-linked associated O-linked sialosyl-2-6 alpha-*N*-acetylgalactosaminyl (sialosyl-Tn) epitope. Cancer Res 1988;48:2214–20.
15. Kurosaka A, Kitagawa H, Fukui S, Numata Y, Nakada H, Funakoshi I, Kawasaki T, Ogawa T, Iijima H, Yamashina I. A monoclonal antibody that recognizes a cluster of a disaccharide, NeuAca2-6GalNAc, in mucin-type glycoproteins. J Biol Chem 1988;263:8724–6.
16. Ito A, Levery SB, Saito S, Satoh M, Hakomori S. A novel ganglioside isolated from renal cell carcinoma. J Biol Chem 2001;276:16695–703.
17. Saito S, Egawa S, Endoh M, Ueno S, Ito A, Numahata K, Satoh M, Kuwao S, Baba S, Hakomori S Arai Y. RM2 antigen (beta1,4-GalNAc-disialyl-Lc4) as a new marker for prostate cancer. Int J Cancer 2005;115:105–13.
18. Langlois MR, Delanghe JR. Biological and clinical significance of haptoglobin polymorphism in humans. Clin Chem 1996;42:1589–600.
19. Turner GA. Haptoglobin. A potential reporter molecule for glycosylation changes in disease. Adv Exp Med Biol 1995;376:231–8.
20. Mineki R, Taka H, Fujimura T, Kikkawa M, Shindo N, Murayama K. *In situ* alkylation with acrylamide for identification of cysteinyl residues in proteins during one- and two-dimensional sodium dodecyl sulphate-polyacrylamide gel electrophoresis. Proteomics 2002;2:1672–81.
21. Liau CY, Chang TM, Pan JP, Chen WL, Mao SJ. Purification of human plasma haptoglobin by hemoglobin-affinity column chromatography. J Chromatogr B Analyt Technol Biomed Life Sci 2003;790:209–16.
22. Brune DC. Alkylation of cysteine with acrylamide for protein sequence analysis. Anal Biochem 1992;207:285–90.
23. Nishimura S, Niikura K, Kurogochi M, Matsushita T, Fumoto M, Hinou H, Kamitani R, Nakagawa H, Deguchi K, Miura N, Monde K, Kondo H. High-throughput protein glycomics: combined use of chemoselective glycoblotting and MALDI-TOF/TOF mass spectrometry. Angew Chem Int Ed Engl 2004;44:91–6.
24. Shimaoka H, Kuramoto H, Furukawa J, Miura Y, Kurogochi M, Kita Y, Hinou H, Shinohara Y, Nishimura S. One-pot solid-phase glycoblotting and probing by transoximization for high-throughput glycomics and glycoproteomics. Chemistry 2007;13:1664–73.
25. Furukawa J, Miura Y, Kuramoto H, Shimaoka H, Kurogochi M, Nakano M, Shinohara Y, Nishimura S. Combined use of hydrazide functionalized polymer and sequential tag exchange: a general protocol with glycoblotting for functional glycomics (part 2) [Abstract no.1185]. Glycobiology 2006;16:1139.
26. Miura Y, Shinohara Y, Furukawa JI, Nagahori N, Nishimura SI. Rapid and simple solid-phase esterification of sialic acid residues for quantitative glycomics by mass spectrometry. Chemistry 2007;13:4797–4804.
27. Uematsu R, Furukawa J, Nakagawa H, Shinohara Y, Deguchi K, Monde K, Nishimura S. High throughput quantitative glycomics and glycoform-focused proteomics of murine dermis and epidermis. Mol Cell Proteomics 2005;4:1977–89.
28. Wada Y, Tajiri M, Yoshida S. Hydrophilic affinity isolation and MALDI multiple-stage tandem mass spectrometry of glycopeptides for glycoproteomics. Anal Chem 2004;76:6560–5.
29. Sutton-Smith M, Dell A. Cell biology: a laboratory handbook. San Diego, CA: Academic Press, 2005.
30. Thompson S, Turner GA. Elevated levels of abnormally-fucosylated haptoglobins in cancer sera. Br J Cancer 1987;56:605–10.
31. Thompson S, Dargan E, Griffiths ID, Kelly CA, Turner GA. The glycosylation of haptoglobin in rheumatoid arthritis. Clin Chim Acta 1993;220:107–14.
32. Hay ED. The mesenchymal cell, its role in the embryo, and the remarkable signaling mechanisms that create it. Dev Dyn 2005;233:706–20.
33. Lee JM, Dedhar S, Kalluri R, Thompson EW. The epithelial-mesenchymal transition: new insights in signaling, development, and disease. J Cell Biol 2006;172:973–81.
34. Blanchard D, Cartron JP, Fournet B, Montreuil J, van Halbeek H, Vliegenthart JF. Primary structure of the oligosaccharide determinant of blood group Cad specificity. J Biol Chem 1983;258:7691–5.
35. Boffey J, Nicholl D, Wagner ER, Townson K, Goodyear C, Furukawa K, Conner J, Willison HJ. Innate murine B cells produce anti-disialosyl antibodies reactive with Campylobacter jejuni LPS and gangliosides that are polyreactive and encoded by a restricted set of unmutated V genes. J Neuroimmunol 2004;152:98–111.
36. Kossowska B, Ferens-Sieczkowska M, Gancarz R, Passowicz-Muszynska E, Jankowska R. Fucosylation of serum glycoproteins in lung cancer patients. Clin Chem Lab Med 2005;43:361–9.
37. Ang IL, Poon TC, Lai PB, Chan AT, Ngai SM, Hui AY, Johnson PJ, Sung JJ. Study of serum haptoglobin and its glycoforms in the diagnosis of hepatocellular carcinoma: a glycoproteomic approach. J Proteome Res 2006;5:2691–700.
38. Ahmed N, Barker G, Oliva KT, Hoffmann P, Riley C, Reeve S, Smith AI, Kemp BE, Quinn MA, Rice GE. Proteomic-based identification of haptoglobin-1 precursor as a novel circulating biomarker of ovarian cancer. Br J Cancer 2004;91:129–40.
39. Bharti A, Ma PC, Maulik G, Singh R, Khan E, Skarin AT, Salgia R. Haptoglobin alpha-subunit and hepatocyte growth factor can potentially serve as serum tumor biomarkers in small cell lung cancer. Anticancer Res 2004;24:1031–8.
40. Okuyama N, Ide Y, Nakano M, Nakagawa T, Yamanaka K, Moriwaki K, Murata K, Ohigashi H, Yokoyama S, Eguchi H, Ishikawa O, Ito T, et al. Fucosylated haptoglobin is a novel marker for pancreatic cancer: a detailed analysis of the oligosaccharide structure and a possible mechanism for fucosylation. Int J Cancer 2006;118:2803–8.
41. Easton RL, Patankar MS, Clark GF, Morris HR, Dell A. Pregnancy-associated changes in the glycosylation of tamm-horsfall glycoprotein. Expression of sialyl Lewis (x) sequences on core 2 type O-glycans derived from uromodulin. J Biol Chem 2000;275:21928–38.
42. Buck CA, Glick MC, Warren L. Effect of growth on the glycoproteins from the surface of control and Rous sarcoma virus transformed hamster cells. Biochemistry 1971;10:2176–80.
43. Ogata S, Muramatsu T, Kobata A. New structural characteristic of the large glycopeptides from transformed cells. Nature 1976;259:580–2.
44. Yamashita K, Ohkura T, Tachibana Y, Takasaki S, Kobata A. Comparative study of the oligosaccharides released from baby hamster kidney cells and their polyoma transformant by hydrazinolysis. J Biol Chem 1984;259:10834–40.
45. Seelentag WKF, Li W-P, Schmitz S-FH, Metzger U, Aeberhard P, Heitz PU, Roth J. Prognostic value of b1,6-branched oligosaccharides in human colorectal carcinoma. Cancer Res 1998;58:5559–64.
46. Cummings RD, Kornfeld S. Characterization of structural determinants required for the high-affinity interaction of asparagine-linked oligosaccharides with immobilized Phaseolus vulgaris leukoagglutinating and erythroagglutinating lectins. J Biol Chem 1982;257:11230–4.
47. Bierhuizen MF, Tedzes H, Schiphorst WE, van den Eijnden DH, van Dijk W. Effect of a2–6-linked sialic acid and a1–3-linked fucose on the interaction of N-linked glycopeptides and related oligosaccharides with immobilized Phaseolus vulgaris leukoagglutinating lectin (L-PHA). Glycoconj J 1988;5:85–97.
48. Schachter H. Biosynthetic controls that determine the branching and microheterogeneity of protein-bound oligosaccharides. Biochem Cell Biol 1986;64:163–81.
49. Kang R, Saito H, Ihara Y, Miyoshi E, Koyama N, Sheng Y, Taniguchi N. Transcriptional regulation of the *N*-acetylglucosaminyltransferase V gene in human bile duct carcinoma cells (HuCC-T1) is mediated by Ets-1. J Biol Chem 1996;271:26706–12.
50. Pierce M, Buckhaults P, Chen L, Fregien N. Regulation of *N*-acetylglucosaminyltransferase V and Asn-linked oligosaccharide beta(1,6) branching by a growth factor signaling pathway and effects on cell adhesion and metastatic potential. Glycoconj J 1997;14:623–30.

ARTICLE IN PRESS

Available online at www.sciencedirect.com

ScienceDirect

ELSEVIER

Biochemical and Biophysical Research Communications xxx (2007) xxx–xxx

BBRC

www.elsevier.com/locate/ybbrc

Tyk2 expression and its signaling enhances the invasiveness of prostate cancer cells

Hisamitsu Ide [a], Takashi Nakagawa [a], Yuichi Terado [b], Yutaka Kamiyama [a], Satoru Muto [a], Shigeo Horie [a,*]

[a] *Department of Urology, Teikyo University School of Medicine, 2-11-1 Kaga, 2chome, Itabashi-ku, Tokyo 173-8605, Japan*
[b] *Department of Pathology, Kyorin University School of Medicine, Mitaka-city, Tokyo, Japan*

Received 13 August 2007

Abstract

Protein tyrosine kinase plays a central role in the proliferation and differentiation of various types of cells. One of these protein kinases, Tyk2, a member of the Jak family kinases, is known to play important roles in receptor signal transduction by interferons, interleukins, growth factors, and other hormones. In the present study, we investigated Tyk2 expression and its role in the growth and invasiveness of human prostate cancer cells. We used a small interfering RNA targeting Tyk2 and an inhibitor of Tyk2, tyrphostin A1, to suppress the expression and signaling of Tyk2 in prostate cancer cells. We detected mRNAs for Jak family kinases in prostate cancer cell lines by RT-PCR and Tyk2 protein in human prostate cancer specimens by immunohistochemistry. Inhibition of Tyk2 signaling resulted in attenuation of the urokinase-type plasminogen activator-enhanced invasiveness of prostate cancer cells *in vitro* without affecting the cellular growth rate. These results suggest that Tyk2 signaling in prostate cancer cells facilitate invasion of these cells, and interference with this signaling may be a potential therapeutic pathway.

Keywords: Tyk2; Jak; Prostate cancer; Invasion; Metastasis

Prostate cancer arises as a consequence of an imbalance between cell division and differentiation. The proliferation, differentiation, growth, and apoptosis of normal and malignant cells are regulated by many different cytokines and growth factors. Protein tyrosine kinases (PTKs) play a central role in the proliferation and differentiation of various types of cells. They participate in the cellular responses to growth factors, and activation of their protein kinase activity is critical for the transmission of mitogenic signals. In a previous study, to explore the function of PTKs in the developing prostate gland, we screened for PTKs expressed in CD44-positive cells from the developing mouse prostate. CD44 is a cell surface glycoprotein receptor and this signaling regulates several important biologic processes including lymphocyte homing and activation, hematopoiesis, and tumor progression and metastasis [1]. In addition, CD44 is expressed during mouse prostate development but not in the adult prostate. Treatment with neutralizing antibodies to CD44 inhibits androgen-stimulated ductal branching morphogenesis in serum-free organ cultures of the mouse prostate [2]. Therefore, CD44 is one of the markers of early progenitor cells in prostate tissues. Using CD44 as a cell surface marker, we isolated several PTK genes including Tyk2 from CD44-positive prostate cells [3].

To date, four mammalian members of the Jak family have been identified, namely, Tyk2, Jak1, Jak2, and Jak3. Previous reports from other laboratories have also demonstrated that Jaks are expressed in a human prostate cancer xenograft model and in bone marrow metastases [4,5]. Extensive studies over the last few years have suggested

Abbreviations: Jak, Janus kinase; RT-PCR, reverse transcriptase-polymerase chain reaction; SH2, Src homology 2; Stat, signal transducers and activators of transcription.

* Corresponding author. Fax: +81 3 3964 8934.
E-mail address: shorie@med.teikyo-u.ac.jp (S. Horie).

0006-291X/$ - see front matter © 2007 Elsevier Inc. All rights reserved.
doi:10.1016/j.bbrc.2007.08.160

Please cite this article in press as: H. Ide et al., Tyk2 expression and its signaling enhances the invasiveness ..., Biochem. Biophys. Res. Commun. (2007), doi:10.1016/j.bbrc.2007.08.160

that Jak kinases play important roles in the responses to interferons, interleukins, growth factors, hormones, and urokinase-type plasminogen activator (uPA), also known as urokinase [6,7]. Activation of Jaks leads to the tyrosine phosphorylation of receptors, producing docking sites for various SH2-containing signaling molecules including Stat proteins [8]. It is well documented that Stats are over-activated in some malignancies. For example, Stat3 activity is elevated in prostate cancer [9]. Accumulating evidence for constitutive activation of various Stats and other oncoproteins in different cancers strongly suggests that Jak kinases play critical roles in the pathogenesis of many human neoplastic diseases [6].

In this study, we examined the expression and biological significance of Tyk2 in prostate cancer. We show that Tyk2 is involved in uPA-induced cell invasion, which is a measure of the malignant potential of prostate cancer cells. Blockade of Tyk2 signaling by a small interfering RNA (siRNA) or by the PTK inhibitor tyrphostin A1 significantly suppresses the invasiveness of human prostate cancer cells into Matrigel. Our results demonstrate that activation of the Tyk2 signaling pathway is important for the enhancement of prostate cancer cell invasiveness by uPA. Thus, the Tyk2 signaling pathway may be a worthwhile target for therapeutic intervention in prostate cancer.

Materials and methods

Cell culture and reagents. Three human prostate cancer cell lines LNCaP, PC-3, DU145, and TSU-Pr1 (bladder cancer cell line) and MCF-7 (breast cancer cell line) were used in this study. The cells were routinely maintained in RPMI 1640 supplemented with 10% fetal calf serum, 100 units/ml penicillin, and 100 μg/ml streptomycin. Cell growth was assessed using a colorimetric proliferation assay employing the tetrazolium 3-(4,5-dimethylthiazol-2-yl)-5-(3-carboxymethoxyphenyl)-2-(4-sulfophenyl)-2*H* tetrazolium (MTS). Each day, MTS was added, and the absorbance at 490 nm was measured on microplate reader after a 60-min incubation at 37 °C. The siRNA duplex targeting Tyk2 and a control siRNA were purchased from Santa Cruz Biotechnology (Santa Cruz, CA). For transfection with siRNAs, DU145 cells were placed in Opti-MEM I (Invitrogen, Carlsbad, CA) and then transfected using oligofectamine (Invitrogen). Tyrphostin A1 (Sigma–Aldrich, St. Louis, MI), an inhibitor of Tyk2 PTK activity, was used at 100 μM, and the effect of uPA (R&D Systems, Minneapolis, MN) was examined at a concentration of 5 nM.

RT-PCR analyses. For RNA expression analysis, total RNA was extracted from cells using RNA Bee (Tel-Test, Friendswood, TX) according to the manufacturer's protocol. The RNA was then treated with DNAse I to remove contaminating DNA and then reverse transcribed using an oligo-dT primer and Super-Scriptβ reverse transcriptase (Invitrogen) in a volume of 25 μl. The primer sequences were as follows: human Jak1, 5′-AAGTGATGTCCTTACCACA-3′ and 5′-AGCAGCCACAC TCAGGTTCT-3′; human Jak2, 5′-GAGCCTATCGGCATGGAATA-3′ and 5′-ATATCTAACACTGCCATCCC-3′; human Jak3, 5′-CAAACAC CACTCCCTGTCCT-3′ and 5′-TGGGGGTGTTCCTGAAGTAG-3′; Tyk2, 5′-GGATGGCCAGGGGCAGTAAG-3′ and 5′-GGATCTCCTC CTCGGTCGAC-3′; prostate-specific antigen, 5′-GGTCGGCACAGCC TGTTTCA-3′ and 5′-CCACGATGGTGTCCTTGATC-3′; β-actin, 5′-GACTACCTCATGAAGATCCT-3′ and 5′-GCGGATGTCCACGTCA CACT-3′. The resulting cDNA was subjected to PCR.

Immunoblot analyses. The cells were washed twice with cold PBS, and lyzed on ice in 2× sample buffer (125 mmol/L Tris, pH 6.8, 4% SDS, 10% 2-β mercaptoethanol, 20% glycerol, 0.06% bromophenol blue). The cell lysates were boiled for 3 min and resolved by 10% SDS–PAGE. Proteins were transferred onto a PVDF membrane (Bio-Rad, Hercules, CA), and immunoblotting was performed using rabbit anti-human Tyk2 antibody (Santa Cruz Biotechnology; 1:1000) or rabbit anti-human β-tubulin antibody (Santa Cruz Biotechnology) as an internal loading control. Goat anti-rabbit antibody conjugated by HRP (Bio-Rad, 1:3000 dilution) were used as a secondary antibody. Immunoreactive proteins were visualized with ECL detection reagents (Amersham Biosciences, Piscataway, NJ).

Immunohistochemistry. Serial 4-mm-thick sections were deparaffinized in three changes of xylene and rehydrated through a graded series of ethanol decreasing from 100% to 70%. The sections were immersed in citrate buffer (pH. 6.0) and autoclaved at 120 °C for 5 min and then placed in 3% hydrogen peroxide in methanol for 20 min at room temperature to block endogenous peroxidase activity. Nonspecific protein binding was blocked by incubating the section for 30 min–1 h in 5% goat serum. Next, the sections were incubated overnight at 4 °C in polyclonal rabbit Tyk2 antibody (Santa Cruz Biotechnology). Sections were then processed for immunohistochemistry using the EnVisionTM+ system (DAKO, Denmark). We examined 70 samples from prostate cancer patients.

Matrigel invasion assay. Membrane inserts (8-μm pore size) for 24-well transwell plates were prepared by coating with Matrigel basement membrane matrix (BD Biosciences, San Jose, CA) according to the manufacturer's instructions. DU145 cells were placed in the upper chamber at a density of 2×10^4 cells/insert. Medium containing 5 nM uPA (R&D Systems, Minneapolis, MN) was added to the lower chamber as a chemoattractant. To inhibit the invasion, 200 nM of Tyk2 siRNA/200 nM oligofectamine or 100 μM of tyrphostin A1 was added to the medium. After 24 h, the upper surface of the inserts was wiped with cotton swabs, and the inserts were stained with Trypan blue. Cells that migrated through the Matrigel and the filter pores to the lower surface were counted in five random high-power fields per insert using a light microscope.

Results

Expression analyses of Tyk2 in prostate cancer cell lines and tissues

We first analyzed the expression of Jaks in MCF-7, LNCaP, PC-3, TSU-Pr1 and DU145 cells by RT-PCR (Fig. 1A). Amplified products for four members of the Jak family, Tyk2, Jak1, Jak2, and Jak3, were clearly detected in these cell lines. We also found that prostate-specific antigen was expressed by LNCaP cells which is androgen sensitive prostate cancer cell line as previously described [3]. Although we tested one androgen sensitive prostate cancer cell line LNCaP, there was no difference of the expression level of Jaks mRNAs between androgen sensitive cells and insensitive cells. We next examined the expression of Tyk2 in human prostate cancer tissue specimens by immunohistochemistry with rabbit anti-human Tyk2 antiserum. The reactivity for Tyk2, shown as brown color, was higher in cancerous than in noncancerous glands in the same field (Fig. 1B). The staining for Tyk2 was heterogeneous and predominately located in the cytoplasm of prostate cancer cells. Of 70 samples from prostate cancer patients, Tyk2 staining was clearly detected in 17 (24.3%). Further studies are needed to accurately determine the correlation between Tyk2 expression in the cancerous tissues and clinical and pathological variables.

Please cite this article in press as: H. Ide et al., Tyk2 expression and its signaling enhances the invasiveness ..., Biochem. Biophys. Res. Commun. (2007), doi:10.1016/j.bbrc.2007.08.160

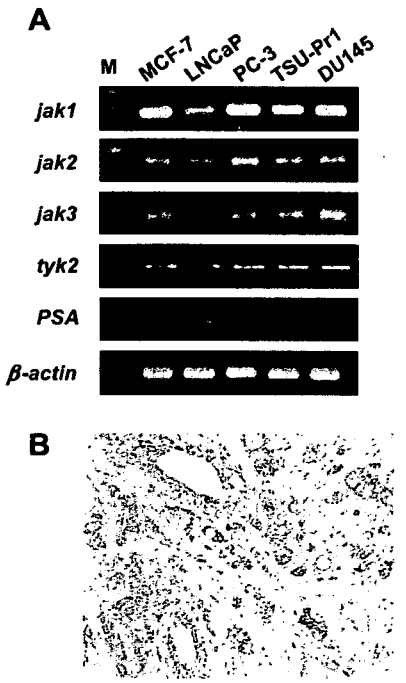

Fig. 1. (A) RT-PCR analysis of Jak family kinases mRNA levels in prostate cancer cell lines. MCF-7 is a breast cancer-derived cell line. (B) Immunohistochemical analysis of Tyk2 expression in prostate cancer tissues. Strong staining is observed in cancerous cells. Histopathological evaluation was done by a pathologist (Y.T.) and hematoxylin and eosin staining shows malignant features of these cells (data not shown).

Interference of Tyk 2 signaling dose not inhibit proliferation of prostate cancer cells

We next examined the role of Tyk2 in cell proliferation using a 96-well-based MTS assay. The experiments were carried out with cells at several different passages and with different batches of transfected cells. At a concentration of 100 μM, tyrphostin A1, a tyrosine kinase inhibitor, did not inhibit the growth rate of DU145 cells (Fig. 2A). Down-regulation of Tyk2 expression using a siRNA also did not inhibit the growth rate of DU145 cells, even though the expression of Tyk2 was decreased (Fig. 2B). These results suggest that signaling by Tyk2 does not affect the proliferation of DU145 cells. Finally, uPA did not affect the growth rate of DU145 cells (Fig. 2C).

Tyk2 signaling involved in invasiveness of prostate cancer cells through uPA

Recent reports suggest that Tyk2 regulates cell migration by mediating uPA activation of phosphatidylinositol 3-kinase [10]. Although uPA is known to regulate the invasiveness of prostate cancer cells, the underlying molecular mechanisms are still unclear. To determine whether Tyk2 participates in the promotion of invasiveness by uPA, we performed Matrigel invasion chamber assays. DU-145 cells were placed in transwells containing Matrigel-coated porous

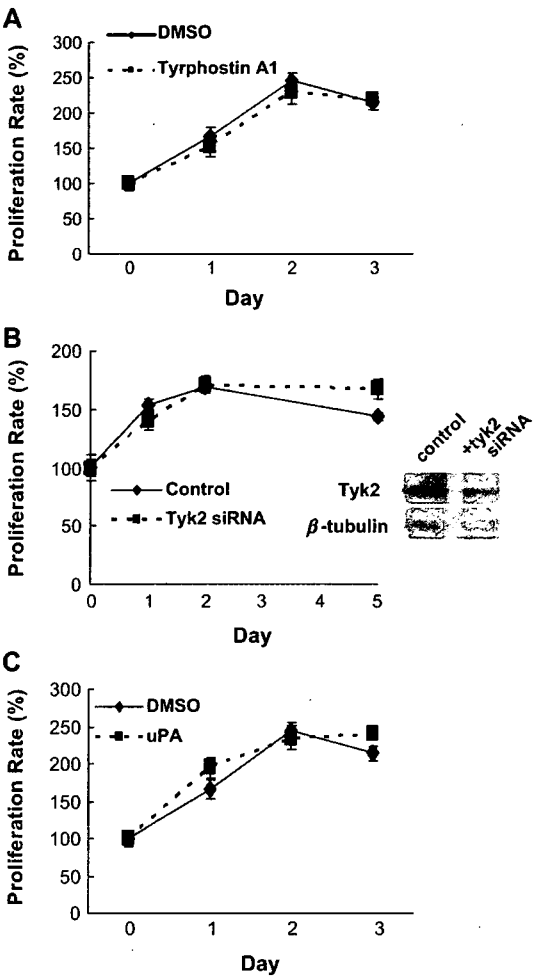

Fig. 2. Role of Tyk2 signaling in the growth of DU145 cells. (A) Tyrphostin A1 did not affect the growth of DU145 cells. (B) The siRNA targeting Tyk2 also did not affect the growth of DU145 cells. (C) uPA did not change a proliferation rate of DU-145 cells. The number of live cells was determined by MTS assay. These assays were repeated two times with different batches of transfected cells, and each cell sample was done in triplicate.

membranes, and the lower chamber was filled with medium with or without uPA. After 24 h, cells that migrated through the Matrigel basement membrane matrix and the filter pores to the lower surface of the membrane were counted by light microscopy. Treatment of cells with tyrphostin A1 inhibited the invasiveness in the presence or absence of uPA in the lower chamber of the transwell (Fig. 3A). In addition, cells transfected with the Tyk2 siRNA, showed decreased invasiveness compared to cells transfected with control siRNA (Fig. 3B). The results with the Tyk2 inhibitor and using the siRNA indicated that inhibition of Tyk2 signaling reduces the invasiveness of prostate cancer cells *in vitro*.

Discussion

In prostate cells, transformation, tumorigenesis, and metastasis can be caused by alterations in cellular regulation,

Please cite this article in press as: H. Ide et al., Tyk2 expression and its signaling enhances the invasiveness..., Biochem. Biophys. Res. Commun. (2007), doi:10.1016/j.bbrc.2007.08.160

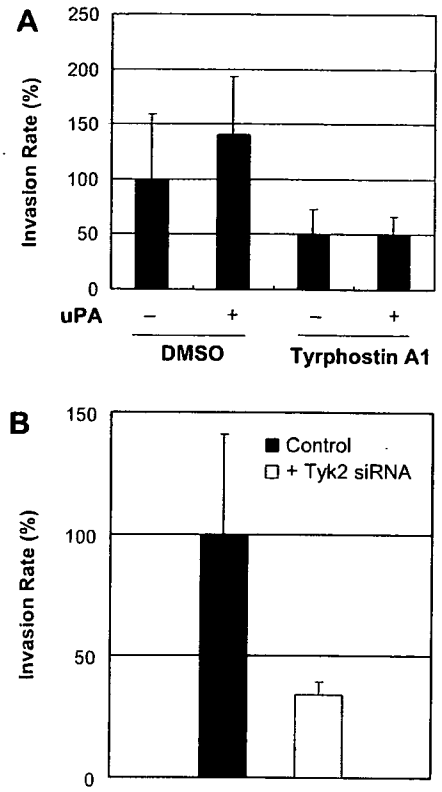

Fig. 3. The enhancement of invasion by uPA is suppressed by blockade of Tyk2 signaling in DU-145 cells. (A) The enhancement of invasiveness by uPA was suppressed by tyrphostin A1, an inhibitor of Tyk2 phosphorylation, in DU145 cells. (B) Down-regulation of Tyk2 expression with a siRNA inhibited the invasiveness of uPA-treated DU145 cells. Assays examining the effect of siRNA were repeated three times with different batches of transfected cells.

especially by dysregulation of signaling by PTKs, including receptors for transforming growth factorα, epidermal growth factor, insulin-like growth factor 1, fibroblast growth factors, hepatocyte growth factor, platelet-derived growth factor, nerve growth factors, and interleukin-6 [11]. For example, immunocytochemical analysis has shown that platelet-derived growth factor receptor-α is expressed in bone marrow metastases from prostate tumors [4]. Also, overexpression of HER-2/neu in primary prostate cancer and in metastatic sites of prostate tumors has been detected before and after hormone therapy [12]. In addition, in prostate cancer cells, interleukin-6 enhances cell growth and causes a parallel activation of the Stat3 signaling pathway [13]. Although some of the signaling components have been investigated in prostate cancer cells, only a few of these PTK genes have been shown to influence their invasiveness and metastatic potential.

CD44 has been implicated in a number of important biologic processes, including lymphocyte homing and activation, hematopoiesis, and tumor progression and metastasis [14]. CD44 may be a marker for immature and progenitor cells in prostate tissues. We previously identified Jak1 and Tyk2 using a PCR-based strategy to screen for PTKs in CD44-positive prostate cells [3]. To our knowledge, this is the first report that Tyk2 plays a significant role in mediating the enhancement of prostate cancer invasion by uPA. We found that prostate cancer cells express Jak family kinases, and in the current studies, we concentrated the role of Tyk2. Blockade of Tyk2 expression using a siRNA significantly suppressed the promotion of human prostate cancer cell invasiveness by uPA. In addition, the Tyk2 inhibitor tyrphostin A1 suppressed the invasiveness of human prostate cancer cells. We also showed that tissue samples from prostate cancer patients are positive for Tyk2.

The activation of Tyk2 signaling may depend on upstream events such as the activation of the uPA, interleukin, and interferon receptors. Furthermore, uPA is a multifunctional molecule that acts as both a proteolytic enzyme and a ligand that induces intracellular signaling. The uPA receptor mediates intracellular signaling *via* surface proteins such as integrins, growth factors receptors, and G-protein-coupled membrane proteins [15]. Several reports have shown that Jaks and Stats interfere with multiple signaling cascades, such as the Ras/mitogen-activated protein kinase pathway and activation of phosphatidylinositol 3-kinase and Src kinases [16]. For instance, Tyk2 is required for the activation of Stat3 by uPA in glomerular mesangial cells [17]. In human vascular smooth muscle cells, uPA stimulates migration *via* the uPA receptor signaling complex, which contains the Tyk2 and phosphatidylinositol 3-kinase [10]. Together with these previous findings, our results suggest that Tyk2 is one of the key molecules in mediating uPA receptor signaling in prostate cancer cells.

Our results also suggest that Tyk2 signaling may contribute to the metastasis of prostate cancer. Further studies are needed to determine whether inhibition of Tyk2 attenuates the metastasis of prostate cancer cells in *in vivo*. We are currently examining the correlation between the expression of Tyk2 in prostate cancer and the pathological and clinical variables. Several inhibitors of Jak protein kinase have been developed as molecular-targeted chemotherapeutic agents [18]. Jak kinase generally functions as a modulator at the intersection of multiple signal transduction pathways. Thus, targeting Tyk2 with specific drugs may be useful for therapeutic intervention in prostate cancer.

References

[1] D. Naor, R.V. Sionov, D. Ish-Shalom, CD44: structure, function, and association with the malignant process, Adv. Cancer Res. 71 (1997) 241–319.
[2] P. Gakunga, G. Frost, S. Shuster, G. Cunha, B. Formby, R. Stern, Hyaluronan is a prerequisite for ductal branching morphogenesis, Development 124 (1997) 3987–3997.
[3] H. Ide, D.B. Seligson, S. Memarzadeh, L. Xin, S. Horvath, P. Dubey, M.B. Flick, B.M. Kacinski, A. Palotie, O.N. Witte, Expression of colony-stimulating factor 1 receptor during prostate development and prostate cancer progression, Proc. Natl. Acad. Sci. USA 99 (2002) 14404–14409.
[4] A. Chott, Z. Sun, D. Morganstern, J. Pan, T. Li, M. Susani, I. Mosberger, M.P. Upton, G.J. Bubley, S.P. Balk, Tyrosine kinases expressed in vivo by human prostate cancer bone marrow metastases

Please cite this article in press as: H. Ide et al., Tyk2 expression and its signaling enhances the invasiveness ..., Biochem. Biophys. Res. Commun. (2007), doi:10.1016/j.bbrc.2007.08.160

and loss of the type 1 insulin-like growth factor receptor, Am. J. Pathol. 155 (1999) 1271–1279.
[5] D. Robinson, F. He, T. Pretlow, H.J. Kung, A tyrosine kinase profile of prostate carcinoma, Proc. Natl. Acad. Sci. USA 93 (1996) 5958–5962.
[6] A. Verma, S. Kambhampati, S. Parmar, L.C. Platanias, Jak family of kinases in cancer, Cancer Metastasis Rev. 22 (2003) 423–434.
[7] D. Hebenstreit, J. Horejs-Hoeck, A. Duschl, JAK/STAT-dependent gene regulation by cytokines, Drug News Pers. 18 (2005) 243–249.
[8] K. Yamaoka, P. Saharinen, M. Pesu, V.E. Holt 3rd, O. Silvennoinen, J.J. O'Shea, The Janus kinases (Jaks), Genome Biol. 5 (2004) 253.
[9] J.V. Alvarez, P.G. Febbo, S. Ramaswamy, M. Loda, A. Richardson, D.A. Frank, Identification of a genetic signature of activated signal transducer and activator of transcription 3 in human tumors, Cancer Res. 65 (2005) 5054–5062.
[10] A. Kusch, S. Tkachuk, H. Haller, R. Dietz, D.C. Gulba, M. Lipp, I. Dumler, Urokinase stimulates human vascular smooth muscle cell migration via a phosphatidylinositol 3-kinase-Tyk2 interaction, J. Biol. Chem. 275 (2000) 39466–39473.
[11] D. Djakiew, Dysregulated expression of growth factors and their receptors in the development of prostate cancer, Prostate 42 (2000) 150–160.
[12] I. Osman, H.I. Scher, M. Drobnjak, D. Verbel, M. Morris, D. Agus, J.S. Ross, C. Cordon-Cardo, HER-2/neu (p185neu) protein expression in the natural or treated history of prostate cancer, Clin. Cancer Res. 7 (2001) 2643–2647.
[13] Z. Culig, G. Bartsch, A. Hobisch, Interleukin-6 regulates androgen receptor activity and prostate cancer cell growth, Mol. Cell Endocrinol. 197 (2002) 231–238.
[14] D. Naor, S. Nedvetzki, I. Golan, L. Melnik, Y. Faitelson, CD44 in cancer, Crit. Rev. Clin. Lab. Sci. 39 (2002) 527–579.
[15] F. Blasi, P. Carmeliet, uPAR: a versatile signalling orchestrator, Nat. Rev. Mol. Cell Biol. 3 (2002) 932–943.
[16] A.C. Ward, I. Touw, A. Yoshimura, The Jak–Stat pathway in normal and perturbed hematopoiesis, Blood 95 (2000) 19–29.
[17] N. Shushakova, N. Tkachuk, M. Dangers, S. Tkachuk, J.K. Park, J. Zwirner, K. Hashimoto, H. Haller, I. Dumler, Urokinase-induced activation of the gp130/Tyk2/Stat3 pathway mediates a pro-inflammatory effect in human mesangial cells via expression of the anaphylatoxin C5a receptor, J. Cell Sci. 118 (2005) 2743–2753.
[18] J.E. Thompson, JAK protein kinase inhibitors, Drug News Pers. 18 (2005) 305–310.

Please cite this article in press as: H. Ide et al., Tyk2 expression and its signaling enhances the invasiveness..., Biochem. Biophys. Res. Commun. (2007), doi:10.1016/j.bbrc.2007.08.160